



British
Geological
Survey

2026 seismic hazard maps for the United Kingdom, the Channel Islands, and the UK offshore Exclusive Economic Zone

Multi Hazards and Resilience programme

Open report OR/26/029

BRITISH GEOLOGICAL SURVEY

MULTI HAZARDS AND RESILIENCE PROGRAMME

OPEN REPORT OR/26/029

Keywords

Seismic hazard; United Kingdom; UK waters; North Sea; UK mainland; spectral acceleration; return period.

Bibliographical reference

Mosca, I. 2026. 2026 seismic hazard maps for the United Kingdom, the Channel Islands, and the UK offshore Exclusive Economic Zone. *British Geological Survey Internal Report, OR/26/029*. 52pp.

Copyright in materials derived from the British Geological Survey's work is owned by UK Research and Innovation (UKRI) and/or the authority that commissioned the work. You may not copy or adapt this publication without first obtaining permission. Contact the BGS Intellectual Property Rights Section, British Geological Survey, Keyworth, email ipr@bgs.ac.uk. You may quote extracts of a reasonable length without prior permission, provided a full acknowledgement is given of the source of the extract.

2026 seismic hazard maps for the United Kingdom, the Channel Islands, and the UK offshore Exclusive Economic Zone

I Mosca

BRITISH GEOLOGICAL SURVEY

The full range of our publications is available from the BGS shop at Nottingham and Cardiff (Welsh publications only). Shop online at <https://shop.bgs.ac.uk/>

The London Information Office also maintains a reference collection of BGS publications, including fossils, for consultation.

We publish an annual catalogue of our maps and other publications; this catalogue is available online or from the BGS shop.

The British Geological Survey carries out the geological survey of Great Britain and Northern Ireland (the latter as an agency service for the government of Northern Ireland), and of the surrounding continental shelf, as well as basic research projects. It also undertakes programmes of technical aid in geology in developing countries.

The British Geological Survey is a component body of UK Research and Innovation.

British Geological Survey offices

**Nicker Hill, Keyworth,
Nottingham NG12 5GG**

Tel 0115 936 3100

BGS Central Enquiries Desk

Tel 0115 936 3143

email enquiries@bgs.ac.uk

BGS Sales

Tel 0115 936 3241

email sales@bgs.ac.uk

**The Lyell Centre, Research Avenue South,
Edinburgh EH14 4AP**

Tel 0131 667 1000

email scotsales@bgs.ac.uk

**Natural History Museum, Cromwell Road,
London SW7 5BD**

Tel 020 7589 4090

Tel 020 7942 5344/45

email bgslondonstaff@bgs.ac.uk

**Cardiff University, Main Building, Park Place,
Cardiff CF10 3AT**

Tel 029 2167 4280

**Geological Survey of Northern Ireland, 7th Floor,
Adelaide House, 39-49 Adelaide Street, Belfast, BT2 8FD**

Tel 0289 038 8462

www2.bgs.ac.uk/gsni/

**Natural Environment Research Council, Polaris House,
North Star Avenue, Swindon SN2 1EU**

Tel 01793 411500

Fax 01793 411501

www.nerc.ac.uk

**UK Research and Innovation, Polaris House,
Swindon SN2 1FL**

Tel 01793 444000

www.ukri.org

Website: <https://www.bgs.ac.uk>

Shop online: <https://shop.bgs.ac.uk/>

Foreword

This report updates the hazard maps for peak ground acceleration and spectral acceleration at 0.2 s and 1.0 s with 5% damping for the United Kingdom (UK) onshore, including the Channel Islands, using the 2024 offshore seismic hazard model (Mosca et al., 2024) and a Monte Carlo-based approach for probabilistic seismic hazard assessment. It also adds the seismic hazard maps for spectral acceleration at 0.15 s for the UK, the Channel Islands, and the UK offshore Exclusive Economic Zone.

Acknowledgements

I thank Dr Richard Luckett for the internal review of this report. I am also grateful to the BGS Graphics Team, in particular Craig Woodward, for producing the high-resolution seismic hazard maps for the UK region.

Figures 1-2 and 23-32 were made using the Generic Mapping Tools v.6.4 (www.soest.hawaii.edu/gmt, last accessed June 2024).

Contents

Foreword.....	ii
Acknowledgements	ii
Contents.....	iii
List of abbreviations and symbols.....	vi
Summary.....	vii
1 Introduction.....	1
2 The 2024 offshore seismic hazard model	2
3 Seismic hazard results.....	3
3.1 Hazard maps.....	3
3.2 Site-specific Hazard results	4
4 Conclusions.....	6
Glossary.....	39
References.....	41

FIGURES

Figure 1 Distribution of earthquakes with $M_w \geq 2.0$ within the study area described by the black, thick polygon. The size of the circles is scaled by magnitude. The blue polygon delineates the boundaries of the UK's offshore Exclusive Economic Zone. Yellow stars indicate the location of the sites selected for the site-specific hazard results in Section 3.2. The distribution of the earthquakes and the geometry of the study area are from Mosca et al. (2024).	8
Figure 2 (a) Summary of the SSC logic tree for the 2024 offshore seismic hazard model. The three weights for the depth distribution are for the UK and Ireland, the North Sea and Northern France and Belgium. (b) Summary of the GMC logic tree for the 2024 offshore seismic hazard model. The SSC and GMC logic trees are from Mosca et al. (2024).....	9
Figure 3 Hazard map for PGA for a 95-year return period. The large, black polygon describes the UK offshore EEZ. BGS © UKRI 2026. Contains OS data © Crown copyright and database right 2026.	10
Figure 4 Hazard map for PGA for a 475-year return period. The large, black polygon describes the UK offshore EEZ. BGS © UKRI 2026. Contains OS data © Crown copyright and database right 2026.	11
Figure 5 Hazard map for PGA for a 1100-year return period. The large, black polygon describes the UK offshore EEZ. BGS © UKRI 2026. Contains OS data © Crown copyright and database right 2026.	12
Figure 6 Hazard map for PGA for a 2475-year return period. The large, black polygon describes the UK offshore EEZ. BGS © UKRI 2026. Contains OS data © Crown copyright and database right 2026.	13
Figure 7 Hazard map for PGA for a 5000-year return period. The large, black polygon describes the UK offshore EEZ. BGS © UKRI 2026. Contains OS data © Crown copyright and database right 2026.	14

Figure 8 Hazard map for SA _{0.15 s} for a 95-year return period. The large, black polygon describes the UK offshore EEZ. BGS © UKRI 2026. Contains OS data © Crown copyright and database right 2026.	15
Figure 9 Hazard map for SA _{0.15 s} for a 475-year return period. The large, black polygon describes the UK offshore EEZ. BGS © UKRI 2026. Contains OS data © Crown copyright and database right 2026.	16
Figure 10 Hazard map for SA _{0.15 s} for a 1100-year return period. The large, black polygon describes the UK offshore EEZ. BGS © UKRI 2026. Contains OS data © Crown copyright and database right 2026.	17
Figure 11 Hazard map for SA _{0.15 s} for a 2475-year return period. The large, black polygon describes the UK offshore EEZ. BGS © UKRI 2026. Contains OS data © Crown copyright and database right 2026.	18
Figure 12 Hazard map for SA _{0.15 s} for a 5000-year return period. The large, black polygon describes the UK offshore EEZ. BGS © UKRI 2026. Contains OS data © Crown copyright and database right 2026.	19
Figure 13 Hazard map for SA _{0.20 s} for a 95-year return period. The large, black polygon describes the UK offshore EEZ. BGS © UKRI 2026. Contains OS data © Crown copyright and database right 2026.	20
Figure 14 Hazard map for SA _{0.20 s} for a 475-year return period. The large, black polygon describes the UK offshore EEZ. BGS © UKRI 2026. Contains OS data © Crown copyright and database right 2026.	21
Figure 15 Hazard map for SA _{0.20 s} for a 1100-year return period. The large, black polygon describes the UK offshore EEZ. BGS © UKRI 2026. Contains OS data © Crown copyright and database right 2026.	22
Figure 16 Hazard map for SA _{0.20 s} for a 2475-year return period. The large, black polygon describes the UK offshore EEZ. BGS © UKRI 2026. Contains OS data © Crown copyright and database right 2026.	23
Figure 17 Hazard map for SA _{0.20 s} for a 5000-year return period. The large, black polygon describes the UK offshore EEZ. BGS © UKRI 2026. Contains OS data © Crown copyright and database right 2026.	24
Figure 18 Hazard map for SA _{1.00 s} for a 95-year return period. The large, black polygon describes the UK offshore EEZ. BGS © UKRI 2026. Contains OS data © Crown copyright and database right 2026.	25
Figure 19 Hazard map for SA _{1.00 s} for a 475-year return period. The large, black polygon describes the UK offshore EEZ. BGS © UKRI 2026. Contains OS data © Crown copyright and database right 2026.	26
Figure 20 Hazard map for SA _{1.00 s} for a 1100-year return period. The large, black polygon describes the UK offshore EEZ. BGS © UKRI 2026. Contains OS data © Crown copyright and database right 2026.	27
Figure 21 Hazard map for SA _{1.00 s} for a 2475-year return period. The large, black polygon describes the UK offshore EEZ. BGS © UKRI 2026. Contains OS data © Crown copyright and database right 2026.	28
Figure 22 Hazard map for SA _{1.00 s} for a 5000-year return period. The large, black polygon describes the UK offshore EEZ. BGS © UKRI 2026. Contains OS data © Crown copyright and database right 2026.	29
Figure 23 PGA, SA _{0.15 s} , SA _{0.20 s} , and SA _{1.00 s} hazard curves for sites in Cardiff, Dover, Edinburgh, and London. Solid and dashed lines are the hazard curves computed using the 2024 offshore hazard model and the 2020 national hazard model, respectively.	30

Figure 24 UHS for return periods of 475 years and 2475 years for sites in Cardiff, Dover, Edinburgh, and London. Solid and dashed lines are computed using the 2024 offshore hazard model and the 2020 national hazard model, respectively.	30
Figure 25 Disaggregation of the hazard for the Cardiff site and 475-year return period by magnitude (M_w), Joyner-Boore distance (R_{jb}) and epsilon (ϵ) for (a) PGA, (b) $SA_{0.2s}$, (c) $SA_{0.2s}$, and (d) $SA_{1.0s}$	31
Figure 26 Disaggregation of the hazard for the Cardiff site and 2475-year return period by magnitude (M_w), Joyner-Boore distance (R_{jb}) and epsilon (ϵ) for (a) PGA, (b) $SA_{0.2s}$, (c) $SA_{0.2s}$, and (d) $SA_{1.0s}$	32
Figure 27 Disaggregation of the hazard for the Dover site and 475-year return period by magnitude (M_w), Joyner-Boore distance (R_{jb}) and epsilon (ϵ) for (a) PGA, (b) $SA_{0.2s}$, (c) $SA_{0.2s}$, and (d) $SA_{1.0s}$	33
Figure 28 Disaggregation of the hazard for the Dover site and 2475-year return period by magnitude (M_w), Joyner-Boore distance (R_{jb}) and epsilon (ϵ) for (a) PGA, (b) $SA_{0.2s}$, (c) $SA_{0.2s}$, and (d) $SA_{1.0s}$	34
Figure 29 Disaggregation of the hazard for the Edinburgh site and 475-year return period by magnitude (M_w), Joyner-Boore distance (R_{jb}) and epsilon (ϵ) for (a) PGA, (b) $SA_{0.2s}$, (c) $SA_{0.2s}$, and (d) $SA_{1.0s}$	35
Figure 30 Disaggregation of the hazard for the Edinburgh site and 2475-year return period by magnitude (M_w), Joyner-Boore distance (R_{jb}) and epsilon (ϵ) for (a) PGA, (b) $SA_{0.2s}$, (c) $SA_{0.2s}$, and (d) $SA_{1.0s}$	36
Figure 31 Disaggregation of the hazard for the London site and 475-year return period by magnitude (M_w), Joyner-Boore distance (R_{jb}) and epsilon (ϵ) for (a) PGA, (b) $SA_{0.2s}$, (c) $SA_{0.2s}$, and (d) $SA_{1.0s}$	37
Figure 32 Disaggregation of the hazard for the London site and 2475-year return period by magnitude (M_w), Joyner-Boore distance (R_{jb}) and epsilon (ϵ) for (a) PGA, (b) $SA_{0.2s}$, (c) $SA_{0.2s}$, and (d) $SA_{1.0s}$	38

TABLES

Table 1 PGA, $SA_{0.15s}$, $SA_{0.20s}$, and $SA_{1.00s}$ for Cardiff, Dover, Edinburgh, and London and two return periods.....	5
Table 2 Disaggregation results (by zone) for the four sites in the UK mainland and for PGA, $SA_{0.15s}$, $SA_{0.20s}$, and $SA_{1.00s}$ at 475 and 2475 years. Only zones that contribute more than 5% to the hazard are reported here.....	5

List of abbreviations and symbols

<i>a</i>	Activity rate
<i>b</i>	<i>b</i> -value
BGS	British Geological Survey
BSI	British Standards
CCS	Carbon Capture and Storage
EEZ	Exclusive Economic Zone
FMD	Frequency-magnitude distribution
GMC	Ground motion characterisation
GMPE	Ground Motion Prediction Equation
HTTA	Host-to-target Adjustment
Mmax	Maximum magnitude
Mw	Moment magnitude
PGA	Peak ground acceleration
PMLP	Penalised maximum likelihood procedure
PSHA	Probabilistic seismic hazard assessment
Rjb	Joyner-Boore distance
SA	Spectral acceleration
SA _{0.15 s}	Spectral acceleration at 0.15 s
SA _{0.20 s}	Spectral acceleration at 0.20 s
SA _{1.00 s}	Spectral acceleration at 1.00 s
SSC	Seismic source characterisation
SSM	Seismic source model
SZM	Source Zone Model
UHS	Uniform Hazard Spectra
UK	United Kingdom
Vs30	Time-averaged shear wave velocity for the top 30 m

Summary

This report updates the 2020 national hazard maps (Mosca et al., 2022) and the 2024 offshore hazard maps (Mosca et al., 2024) for peak ground acceleration (PGA) and spectral acceleration (SA) at 0.2 s and 1.0 s with 5% damping for the United Kingdom (UK) onshore, including the Channel Islands, using the 2024 offshore seismic hazard model (Mosca et al., 2024) and a Monte Carlo-based approach for probabilistic seismic hazard assessment. It also includes the seismic hazard maps for an additional SA, i.e. $SA_{0.15\text{ s}}$, for the United Kingdom, the Channel Islands, and the UK offshore Exclusive Economic Zone. The maps described in this report are referred to as “2026 seismic hazard maps”.

After a brief description of the 2024 offshore seismic hazard model, I describe the 2026 seismic hazard maps in the UK region for four ground motion parameters, i.e., peak ground acceleration (PGA), spectral acceleration at 0.15 s ($SA_{0.15\text{ s}}$), 0.2 s ($SA_{0.20\text{ s}}$), and 1.0 s ($SA_{1.00\text{ s}}$), and five return periods (95 years, 475 years, 1100 years, 2475 years, and 5000 years). It is the first time that hazard estimates are provided for a 5000-year return period and the UK onshore. Overall, the 2026 hazard maps confirm that seismic hazard in the UK region is generally low by worldwide hazard standard and increases slightly in regions of higher observed seismic activity, such as North Wales, the Welsh Marches, the northern North Sea, and the southern North Sea around the Dogger Bank area, where the largest (5.9 moment magnitude) instrumentally recorded earthquake occurred. The highest hazard is observed around the region of Snowdonia, in North Wales, and in the northern North Sea. For a 475-year return period, these values are 0.06-0.07 g for PGA, 0.16-0.19 g $SA_{0.15\text{ s}}$, and 0.13-0.16 g for $SA_{0.20\text{ s}}$, and 0.02 g for $SA_{1.00\text{ s}}$; whereas, for 2475 years, they are 0.19-0.21 g for PGA, 0.48-0.52 g $SA_{0.15\text{ s}}$, and 0.39-0.42 g for $SA_{0.20\text{ s}}$ and 0.05 g for $SA_{1.00\text{ s}}$.

The report also includes site-specific hazard results (hazard curves, uniform hazard spectra, disaggregation analysis) for selected locations in the UK mainland (i.e. Cardiff, Dover, Edinburgh, and London) and a comparison of these site-specific results with those published in Mosca et al. (2020, 2022) using the 2020 national seismic hazard model. In general, there is an increase in hazard for all ground motion parameters at all sites, except for the PGA, $SA_{0.15\text{ s}}$, $SA_{0.20\text{ s}}$ hazard curves at Dover. This is due to the differences between the two hazard models, which are discussed extensively in Mosca (In preparation).

The 2026 seismic hazard map for 475 years, and $SA_{0.15\text{ s}}$ is used to calibrate the design seismic requirements of the second-generation Eurocode 8 to the hazard levels of the UK (BS NA EN 1998-1, 2026; PD6698, 2026).

1 Introduction

The British Geological Survey (BGS) developed and published the 2024 offshore seismic hazard models, together with accompanying maps for the UK Exclusive Economic Zone (EEZ), to update the previous maps, which were published in 2002 (EQE Ltd, 2002). The work was funded by the Industrial Decarbonisation Research and Innovation Centre (IDRIC) and was informed at key stages by external experts who reviewed the project's main components. The development of the 2024 offshore hazard model and maps addressed some of the limitations of the 2020 national seismic hazard model for the UK (Mosca et al., 2022). Therefore, the 2024 offshore model represents an improvement to the 2020 national hazard model, incorporating the latest data and advances in probabilistic seismic hazard assessment (PSHA) methodologies.

The goal of the 2024 offshore maps was to provide a robust indication of the level of seismic hazard to underpin the planning and design of offshore structures and carbon capture and storage (CCS) sites in UK waters, e.g., Acorn CCS site in the Moray Firth Basin and HyNet North West CCS area in the Irish Sea. They also help identify regions of high seismic hazard to inform the need for site-specific risk assessments and provide a robust baseline for tectonic seismic activity in UK waters, which can be used to help discriminate any seismicity induced by operations, such as CCS, in the event it occurs. Unlike the 2020 national seismic hazard maps of Mosca et al. (2022), which were developed to guide the application of the second-generation Eurocode 8 (BS NA EN 1998-1 2026) in the UK and thus to calibrate the seismic design requirements, the 2024 offshore maps were intended to be used only for offshore engineering structures. For this reason, the 2024 offshore maps in Mosca et al. (2024) do not show the hazard of onshore UK.

Unlike the first-generation Eurocode 8, where the elastic seismic design requirements were anchored to peak ground acceleration (PGA) for a 475-year return period (EN1998, 2005), in the second-generation Eurocode 8, these are anchored to the spectral acceleration (SA) at short periods and at 1.0 s for 475 years (EN1998, 2026). The exact value for the short period is a Nationally Determined Parameter, defined by each country, and corresponds to the peak of the Uniform Hazard Spectra (UHS). Following guidance from the British Standards Institution (BSI) committee B/525/8 for Structures in Seismic Regions (the committee responsible for the UK input to Eurocode 8), this value was agreed to be 0.2 s for the UK in 2018. However, in February 2026, the BSI committee B/525/8 reviewed this decision based on further analysis of the elastic seismic design requirements of the second-generation Eurocode 8 and indicated that the use of spectral acceleration at 0.15 s, rather than 0.20 s, is a better choice for the UK. Moreover, BSI committee B/525/8 decided to use the 2024 offshore hazard maps, rather than the 2020 onshore national seismic hazard maps, to calibrate the seismic action requirements in the second-generation Eurocode 8 to the UK seismic hazard levels. This decision was driven by the fact that the 2024 offshore seismic hazard model was developed to account for some limitations of the 2020 onshore national hazard model, slightly updated data and recent advances in seismic hazard methodology, such as a separate aleatory model for the ground motion.

The present report expands the Mosca et al. (2024) BGS report to publish the 2024 seismic hazard maps for the UK, the Channel Islands, and the UK offshore Exclusive Economic Zone, for four ground motion parameters, i.e., PGA, spectral acceleration at 0.15 s ($SA_{0.15\text{ s}}$), 0.2 s ($SA_{0.20}$), and 1.0 s ($SA_{1.00\text{ s}}$), together with site-specific hazard results for the same ground motion parameters and selected locations in the UK mainland. In Section 2, I give a general overview of the 2024 offshore seismic hazard model. However, the reader can refer to Mosca et al. (2024) for further information on its development. Section 3 describes the seismic hazard maps in the UK region, which are referred to as “2026 hazard maps”, and the site-specific hazard results across the UK. A quantitative comparison of the 2026 and 2020 national hazard maps, together with the factors driving the difference in hazard between the two models, will be included in a peer-reviewed publication (Mosca, in preparation). Section 4 provides general conclusions.

2 The 2024 offshore seismic hazard model

The offshore seismic hazard model comprises the region up to 300 km from the UK offshore EEZ, which is the 200-mile zone around the UK coastline (Gibson, 2009; red polygon in Figure 1). This region accounts for all seismic sources which may influence the hazard in UK waters since earthquakes beyond 300 km from a site are unlikely to affect the hazard (e.g. IAEA, 2022).

To develop the offshore seismic source model, a comprehensive catalogue of earthquake activity across the study area was built by combining existing earthquake catalogues and data from regional and local monitoring agencies. Anthropogenic events, such as blasting, underwater explosions, mining and hydrocarbon exploration, have been removed where possible. We also removed foreshocks and aftershocks to ensure that the catalogue only contains time-independent events. Then, published empirical magnitude conversion relationships were used to convert different magnitude scales to moment magnitude (M_w) and thus ensure that the catalogue has consistent and homogeneous magnitudes across the region of interest. Finally, the catalogue completeness was assessed for different time intervals using both published information for the earthquake catalogues from the region and by examining cumulative and annual numbers of earthquakes for specific magnitudes. The reader can refer to Mosca et al. (2024) for further information on how the data from various sources were prioritised and the decision to develop the declustering and completeness analysis of the catalogue. Figure 1 shows the distribution of seismicity, which consists of 4753 tectonic earthquakes (mainshocks and time-dependent events; grey circles in Figure 1) and 4018 mainshocks (red circles in Figure 1) with $M_w \geq 2.0$ from the year 1000 to 31 December 2022 within the study area.

The seismic source characterisation (SSC) model consists of four different seismic source zone models (SZM1-SZM4; see Figures 18-21 in Mosca et al., 2024) to capture the epistemic uncertainty in different rupture scenarios. Specific fault sources were not included in the SSC model because of the difficulty relating earthquakes to particular faults in the region of interest. SZM1 is strongly based on the main structural domains and the distribution of seismicity. It corresponds to the SSC model developed for the 2020 national seismic hazard model for the UK (Mosca et al., 2022) and the source model for northern France, Belgium, the North Sea, and the Atlantic Ocean used in the 2020 European seismic hazard model (Danciu et al., 2024). SZM2 is based on the geological and structural understanding of the region, focusing on zones that are consistent with the known geological structures. This includes rocks of similar type which have been subjected to the same deformation events and, therefore, have similar structural trends and should behave similarly in a given stress field. Models SZM3-SZM4 are the two seismic source models used in the previous offshore hazard study by EQE Ltd (2002). Each zone of the SZMs is described in terms of the geometry, the earthquake recurrence statistics for the seismicity in the zone, the maximum and minimum magnitudes, the distribution of the hypocentral depths, and the faulting style.

Figure 2a summarises the logic tree used for the SSC model for the 2024 offshore seismic hazard model. We used a four-value (6.5 - 7.1 M_w) maximum magnitude (M_{max}) distribution, which was adopted for the national seismic hazard models for the UK (Mosca et al., 2022), for all four SZMs. We quantified the frequency-magnitude distribution (FMD) for each seismic source zone of the four SZMs using the earthquake catalogue derived for the study and the penalised maximum likelihood procedure (PMLP; Johnston et al., 1994). The results from the PMLP are expressed by a 5×5 matrix of possible values for the recurrence parameters (i.e. the activity rate a and the b -value), determining 25 triplets of a and b and their weight to account for the uncertainty in these parameters. The hypocentral depths of the earthquakes in the study area are distributed throughout the upper 25 km of the crust, with events along the Norwegian coast area being slightly deeper than those in the UK and northern France. Given the stress conditions in the study area, it is assumed here that future significant earthquakes are in agreement with calculated fault plane solutions for instrumentally recorded earthquakes in the last 30 years. For example, for the zones in the British Isles, they will be most likely to be strike-slip faulting events with N-S to NW-SE compression and E-W to NE-SW tension (Baptie 2010); whereas, the earthquakes are expected to be either strike-slip or reverse faulting with equally weighted N-S or NW-SE orientations in the North Sea and Norway (Lindhölm et al., 2000; Ottemöller et al., 2005).

An overview of the logic trees used for the ground motion characterisation (GMC) model of the 2024 offshore seismic hazard model is shown in Figure 2b. We selected a suite of five recently published ground motion prediction equations (GMPEs; i.e. Abrahamson et al., 2014; Bindi et al., 2014; Cauzzi et al., 2015; Yenier et al., 2015; and Rietbrock and Edwards, 2019 for 10MPa), which we considered applicable to the study area. The GMPEs are included in a logic tree where the weights are informed by the fit between observed and modelled ground motions and discussion within the project team. This suite of ground motion models is an update of the ground motion logic tree used in the 2020 national PSHA for the UK (Mosca et al., 2022) where the models of Atkinson and Boore (2006) and Rietbrock et al. (2013) have been superseded by their more recent updates (i.e. Yenier et al., 2015; and Rietbrock and Edwards, 2019). The GMC model also includes the host-to-target adjustments (HTTAs), which account for differences between the host region where the GMPE was derived and the target region where the hazard is being estimated (Douglas and Edwards, 2016), and a single-station sigma model, which describes the aleatory variability in the predicted ground motions (Al Atik, 2015).

3 Seismic hazard results

We applied the Monte Carlo-based approach for PSHA (for an extensive description of this methodology, see Mosca et al., 2024), where the branches in the SSC and GMC logic tree are sampled at random based on their weights. Using the SSC model (top panel in Figure 2a), we generated 1,000,000 synthetic earthquake catalogues, each 100 years long. This gives a total of 100,000,000 years of simulated data, which is sufficient to resolve the hazard accurately for return periods up to 10,000 years (Musson, 2000). The ground motion for each earthquake in the simulated catalogues is computed using the ground motion logic tree in Figure 2b. Sorting the ground motion results in order of decreasing severity allows us to identify ground motions associated with different frequencies of exceedance (Musson, 2000).

3.1 HAZARD MAPS

The 2026 hazard maps cover the UK, the Channel Islands, and the offshore UK EEZ (UK commercial waters), comprising a grid of 4663 points that are spaced 0.125° in latitude and 0.25° in longitude. These maps have been estimated for four ground motion parameters, i.e. the hazard for PGA (Figures 3-7), spectral acceleration at 0.15 s ($SA_{0.15\text{ s}}$; Figures 8-12), 0.2 s ($SA_{0.20\text{ s}}$; Figures 13-17), and 1.0 s ($SA_{1.00\text{ s}}$; Figures 18-22), for 5% damping on rock conditions (time-averaged shear wave velocity for the top 30 m, V_{s30} , of 800 m/s) and for five return periods, 95, 475, 1100, 2475, and 5000 years.

Overall, the 2026 hazard maps confirm that seismic hazard in and around the UK is generally low by worldwide hazard standard and increases slightly in regions of higher observed seismic activity, such as North Wales, the Welsh Marches, the northern North Sea, and the southern North Sea around the Dogger Bank area, where the largest (5.9 Mw) instrumentally recorded earthquake occurred. Specifically, for the 95-year return period, the hazard is less than 0.02 g for PGA and $SA_{1.00\text{ s}}$ (Figures 3 and 18) and increases slightly more for the other two spectral accelerations (up to 0.08 g for $SA_{0.15\text{ s}}$ and 0.06 g for $SA_{0.20\text{ s}}$; Figures 8 and 13).

For 475 years, PGA is less than 0.04 g for most of the UK and offshore regions, except for the northern North Sea east of Shetland, North Wales, the southern North Sea immediately offshore Lincolnshire and East Anglia, and the Welsh Marches in Mid Wales, where the hazard reaches around 0.07 g, 0.06 g, 0.05 g, and 0.04 g, respectively (Figure 4). A similar spatial pattern in the hazard is observed for $SA_{0.15\text{ s}}$ and $SA_{0.20\text{ s}}$ with higher hazard values. The values for $SA_{0.15\text{ s}}$ reach 0.19 g in the northern North Sea, 0.16 g around Snowdonia, 0.13 g in the southern North Sea, and 0.11 g in the Welsh Marches (Figure 9), whereas $SA_{0.20\text{ s}}$ is up to 0.16 g, 0.13 g, 0.11 g, and 0.09 g in the same locations (Figure 14). $SA_{1.00\text{ s}}$ is less than 0.02 g everywhere (Figure 19).

For a return period of 1100 years, we observe a similar spatial variation to the maps for 475 years with the highest hazard again in North Wales (up to 0.12 g for PGA, 0.31 g $SA_{0.15\text{ s}}$, and 0.25 g for $SA_{0.20\text{ s}}$), the northern North Sea (up to 0.12 g for PGA, 0.31 g $SA_{0.15\text{ s}}$, and 0.25 g for $SA_{0.20\text{ s}}$), the southern North Sea (up to 0.10 g for PGA, 0.26 g $SA_{0.15\text{ s}}$, and 0.21 g for $SA_{0.20\text{ s}}$), and the Welsh

Marches (up to 0.08 g for PGA, 0.20 g $SA_{0.15\text{ s}}$, and 0.17 g for $SA_{0.20\text{ s}}$; (Figures 5, 10, and 15). There is much less variation for $SA_{1.00\text{ s}}$ with the highest hazard being less than 0.04 g (Figure 20).

For a return period of 2475 years, North Wales, the northern and southern North Sea, the English-Wales border region through to North Central England, and NW Scotland are the areas of highest hazard for PGA (Figure 6), $SA_{0.15\text{ s}}$ (Figure 11), and $SA_{0.20\text{ s}}$ (Figure 16). The highest hazard values (0.21 g for PGA, 0.52 g $SA_{0.15\text{ s}}$, and 0.42 g for $SA_{0.20\text{ s}}$) are observed around the region of Snowdonia, in North Wales. The highest value for $SA_{1.00\text{ s}}$ (0.052 g) is in the northern North Sea, rather than around Snowdonia (Figure 21).

For the hazard maps at the 5000-year return period, the spatial variation is similar to that in the previous maps with higher hazard values (Figures 7, 12, 17, and 22).

It is worth noting that the region with the highest hazard is the northern North Sea, at the edge of the north-east boundary of the EEZ for return periods shorter than 1100 years, and the North Wales region around Snowdonia for longer return periods than 1100 years. At 1100 years the hazard in these two areas is identical (0.12 g for PGA, 0.31 g $SA_{0.15\text{ s}}$, 0.25 g for $SA_{0.20\text{ s}}$, and 0.03 g $SA_{1.00\text{ s}}$).

3.2 SITE-SPECIFIC HAZARD RESULTS

We have computed the hazard for the same sites used in Mosca et al. (2022). These are Cardiff (51.48°N, -3.18°E), Dover (51.13°N, 1.31°E), Edinburgh (55.95°N, -3.20°E), and London (51.50°N, 0.13°E) and were selected because they have different levels of hazard. Note that site-specific hazard results for locations in UK waters are shown in Mosca et al. (2024). The locations of the sites are indicated in Figure 1. The hazard curves for PGA, $SA_{0.15\text{ s}}$, $SA_{0.20\text{ s}}$, and $SA_{1.00\text{ s}}$ are shown in Figure 23. This figure also shows the comparison of the hazard curves using the 2024 offshore seismic hazard model (solid lines) and those published in Mosca et al. (2022) using the 2020 national seismic hazard model (dashed lines). Note that the hazard curves for the $SA_{0.15\text{ s}}$ have been computed for this updated report using only the 2024 model. The comparison of the hazard curves between the two works shows that there is an increase in hazard for all the ground motion parameters and sites, using the 2024 offshore model, rather than the 2020 model, except for the PGA, $SA_{0.15\text{ s}}$, and $SA_{0.20\text{ s}}$ hazard curves at Dover. For Dover, the decrease in hazard is -21% for PGA and -5% for $SA_{0.20\text{ s}}$ for a 2475-year return period. For Cardiff and 2475 years, the hazard increases up to 9% and 14% for PGA and $SA_{0.20\text{ s}}$, respectively, and decreases by 3% for $SA_{1.00\text{ s}}$. For Edinburgh, the increase in hazard is the highest (41% for PGA, 53% for $SA_{0.20\text{ s}}$ and 34% for $SA_{1.00\text{ s}}$ for 2475 years) among the four sites. Finally, for London, the hazard has an increase between 18% and 37% for a 2475-year return period. The variation in hazard from the 2020 hazard model to the 2024 offshore hazard model is extensively discussed in Mosca (in preparation). Table 1 gives the PGA, $SA_{0.15\text{ s}}$, $SA_{0.20\text{ s}}$, and $SA_{1.00\text{ s}}$ for the four sites and two return periods (475 years and 2475 years).

The uniform hazard spectra (UHS) for 475 years and 2475 years are shown in Figure 24, together with the comparison of the UHS computed using the 2020 and 2024 hazard models. These show the hazard values for different periods of ground motion with an equal probability of exceedance and demonstrate that the hazard values peak between periods of 0.1 and 0.4 s. Using the 2024 hazard model, rather than the 2020 model, the UHS increase for the entire period range and for the two return periods at the four selected sites, except for periods between 0.1 s and 0.3 s and 2475 years at a site in Dover.

The disaggregation results in Figures 25-32 show the contribution to the hazard (in %) for two return periods (475 years and 2475 years) and PGA, $SA_{0.15\text{ s}}$, $SA_{0.20\text{ s}}$, and $SA_{1.00\text{ s}}$ in terms of source zone, Mw, Joyner-Boore distance (R_{jb}), and ϵ . The analysis selects magnitude bins of 0.2 units and distance bins of 10 km. Table 2 shows an overview of the disaggregation results in terms of the zone, indicating only the zones that contribute more than 5% to the hazard, to avoid a lengthy table. Overall, the hazard for PGA, $SA_{0.15\text{ s}}$, $SA_{0.20\text{ s}}$ and the two return periods is dominated by small-to-moderate (4.3-5.0 Mw) earthquakes at relatively close distances (< 35 km) for all four sites. Earthquakes of similar size and distances contribute to the $SA_{1.00\text{ s}}$ hazard for 475 years at a Cardiff site; whereas for 2475 years, the magnitudes of the earthquakes, which dominate $SA_{1.00\text{ s}}$, increase slightly (up to 5.5 Mw) at Cardiff. For the other three sites, a broad

range of moderate-to-large (5.5-6.1 Mw) earthquakes contributes to the $SA_{1.00\text{ s}}$ hazard at large (between 200 and 250 km) distances, except for 2475 years at Edinburgh, where earthquakes of 5.3-5.7 Mw at close (15-35 km) distances contribute mainly to $SA_{1.00\text{ s}}$.

Disaggregating by zones shows that the large contributions come from either zones where the sites fall in or zones with high seismicity levels, which are close to the site. For the Cardiff site, the hazard is dominated by the zones, which include the site (i.e. MMCW1, WRET2, SWAL3, and WACE4) for the two return periods and the four ground motion parameters, with other zones contributing very little to the hazard. Zones in the south-eastern Britain and northern France/Belgium region control the hazard at the Dover site, with the biggest contribution coming from zone DOVE1, BRAM2, LOBR3, and LOBR4. For the Edinburgh site, the largest contributions to the hazard are from zones SC341, ESCO1, HIGL3, and HIGL4. Finally, more zones contribute to the hazard for the London site. These include zones where the site falls in (MMCE1, CHAT2) as well as neighbouring zones with high earthquake activity, such as LOBR3, LOBR4, BRAM2, SOLE2, and SLPT1.

Table 1 PGA, $SA_{0.15\text{ s}}$, $SA_{0.20\text{ s}}$, and $SA_{1.00\text{ s}}$ for Cardiff, Dover, Edinburgh, and London and two return periods.

Site	Return period [yr]	PGA [g]	$SA_{0.15\text{ s}}$ [g]	$SA_{0.20\text{ s}}$ [g]	$SA_{1.00\text{ s}}$ [g]
Cardiff	475	0.035	0.088	0.075	0.011
Cardiff	2475	0.109	0.275	0.229	0.031
Dover	475	0.014	0.036	0.033	0.007
Dover	2475	0.042	0.111	0.096	0.019
Edinburgh	475	0.013	0.033	0.030	0.007
Edinburgh	2475	0.035	0.094	0.083	0.017
London	475	0.013	0.034	0.032	0.007
London	2475	0.037	0.097	0.084	0.018

Table 2 Disaggregation results (by zone) for the four sites in the UK mainland and for PGA, $SA_{0.15\text{ s}}$, $SA_{0.20\text{ s}}$, and $SA_{1.00\text{ s}}$ at 475 and 2475 years. Only zones that contribute more than 5% to the hazard are reported here.

Contribution to hazard [%] for Cardiff								
Zone	PGA		$SA_{0.15\text{ s}}$		$SA_{0.20\text{ s}}$		$SA_{1.00\text{ s}}$	
	475 yr	2475 yr	475 yr	2475 yr	475 yr	2475 yr	475 yr	2475 yr
MMCW21	44.3	46.1	44.1	45.1	45.2	45.5	32.6	41.1
WRET2	13.7	15.9	14.1	13.4	12.9	12.3	7.9	11.7
SWAL23	16.5	21.5	14.8	22.4	15.6	21.5	11.6	14.7
WACE4	11.8	10.6	10.9	11.1	10.5	11.9	9.9	12.2
Other zones	< 5.0	< 5.0	< 5.0	< 5.0	< 5.0	< 5.0	< 5.0	< 5.0

Contribution to hazard [%] for Dover								
Zone	PGA		$SA_{0.15\text{ s}}$		$SA_{0.20\text{ s}}$		$SA_{1.00\text{ s}}$	
	475 yr	2475 yr	475 yr	2475 yr	475 yr	2475 yr	475 yr	2475 yr
DOVE1	6.9	12.9	7.0	13.0	6.5	13.3	2.7	4.6
SLPT1	3.0	0.6	3.2	0.7	3.8	1.2	5.7	4.0
BEL11	7.7	6.6	7.3	6.8	7.0	7.1	4.3	6.2

BRAM2	19.3	20.6	18.3	20.4	18.1	18.9	10.6	15.5
SOLE2	3.1	0.9	3.5	0.7	3.9	1.4	5.5	4.4
LOBR3	7.5	12.0	7.3	12.6	6.5	10.5	2.6	4.5
LOBR4	7.6	13.2	7.3	12.3	6.5	11.8	2.7	4.6
Other zones	< 5.0	< 5.0	< 5.0	< 5.0	< 5.0	< 5.0	< 5.0	< 5.0

Contribution to hazard [%] for Edinburgh

Zone	PGA		SA _{0.15 s}		SA _{0.20 s}		SA _{1.00 s}	
	475 yr	2475 yr	475 yr	2475 yr	475 yr	2475 yr	475 yr	2475 yr
SC341	12.5	14.4	11.9	14.2	11.4	13.3	5.4	8.1
ESCO1	14.2	15.9	14.1	16.6	13.3	14.8	9.0	10.8
HIGL3	13.0	15.3	12.7	15.4	11.8	15.6	6.1	8.5
HIGL4	13.7	18.5	13.6	16.2	12.8	15.6	6.4	9.3
Other zones	< 5.0	< 5.0	< 5.0	< 5.0	< 5.0	< 5.0	< 5.0	< 5.0

Contribution to hazard [%] for London

Zone	PGA		SA _{0.15 s}		SA _{0.20 s}		SA _{1.00 s}	
	475 yr	2475 yr	475 yr	2475 yr	475 yr	2475 yr	475 yr	2475 yr
SLPT1	3.7	1.5	4.3	1.6	4.6	2.6	6.0	4.8
EANG1	4.8	5.3	4.6	5.4	4.4	5.7	2.1	2.5
MMCE1	12.0	22.8	10.9	21.8	10.4	19.4	4.3	7.1
MMCW21	6.0	1.9	6.5	2.4	6.8	3.5	7.5	6.8
CHAT2	5.1	9.8	4.6	9.2	4.3	7.2	1.6	2.8
BRAM2	15.8	17.1	15.2	17.5	14.5	17.2	9.1	12.4
SOLE2	3.5	1.4	4.0	2.4	4.0	1.5	5.3	4.6
LOBR3	5.0	8.2	4.6	7.5	4.1	6.6	1.7	2.7
LOBR4	4.9	7.5	4.7	6.7	4.3	6.7	1.7	3.0
Other zones	< 5.0	< 5.0	< 5.0	< 5.0	< 5.0	< 5.0	< 5.0	< 5.0

4 Conclusions

The present work developed and presented the hazard for SA_{0.15 s} in the UK and the Channel Islands, and the UK EEZ for five return periods (95 years, 475 years, 1100 years, 2475 years, and 5000 years) using the 2024 offshore seismic hazard model described in Mosca et al. (2024). The SA_{0.15 s} hazard map for the 475-year return period is currently used to calibrate the seismic design requirements of the second-generation Eurocode 8 to the UK and thus will be referenced in the updated BSI National Annex (2026) and PD6698 (2026). This report also includes the seismic hazard maps for PGA and spectral acceleration at 0.2 s and 1.0 s across the onshore UK, computed using the 2024 offshore seismic hazard model developed in Mosca et al. (2024), who only showed the maps for UK waters.

The maps shown in this report, which are referred to as “2026 hazard maps”, confirm that seismic hazard in and around the UK is generally low by worldwide hazard standard and increases slightly in regions of higher observed seismic activity, such as North Wales, the Welsh Marches, the northern North Sea, and the southern North Sea around the Dogger Bank area.

I compared the seismic hazard curves and UHS for four sites in the UK mainland using the 2020 national seismic hazard model (Mosca et al., 2022) and the 2024 offshore seismic hazard model. The comparison shows a general increase in the hazard for Cardiff, Edinburgh, and London, and a slight decrease in hazard for Dover. An extensive comparison of the 2020 and 2026 hazard maps and the factors driving such differences will be included in the peer-reviewed paper Mosca (In Preparation).

The 2026 offshore and onshore maps will be accessible to the public at <https://www.earthquakes.bgs.ac.uk/hazard/UKhazard.html> and will be included in the BGS interactive mapping tool Geindex. The mapping tool Geindex (offshore) allows users to view the hazard maps interactively, navigate to a specific area of interest, query the maps, and download the hazard values at a specific location or area of interest.

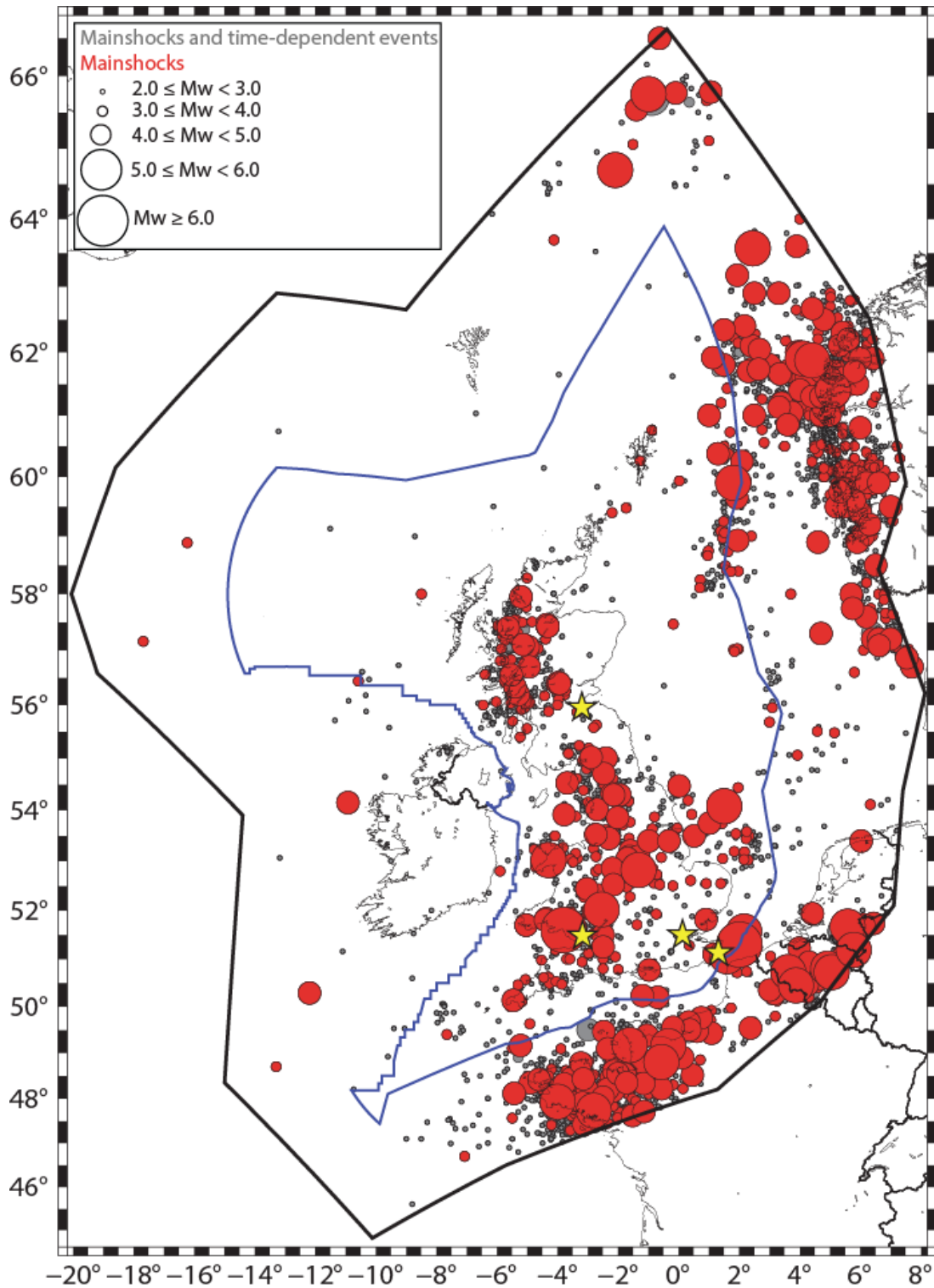


Figure 1 Distribution of earthquakes with $M_w \geq 2.0$ within the study area described by the black, thick polygon. The size of the circles is scaled by magnitude. The blue polygon delineates the boundaries of the UK's offshore Exclusive Economic Zone. Yellow stars indicate the location of the sites selected for the site-specific hazard results in Section 3.2. The distribution of the earthquakes and the geometry of the study area are from Mosca et al. (2024).

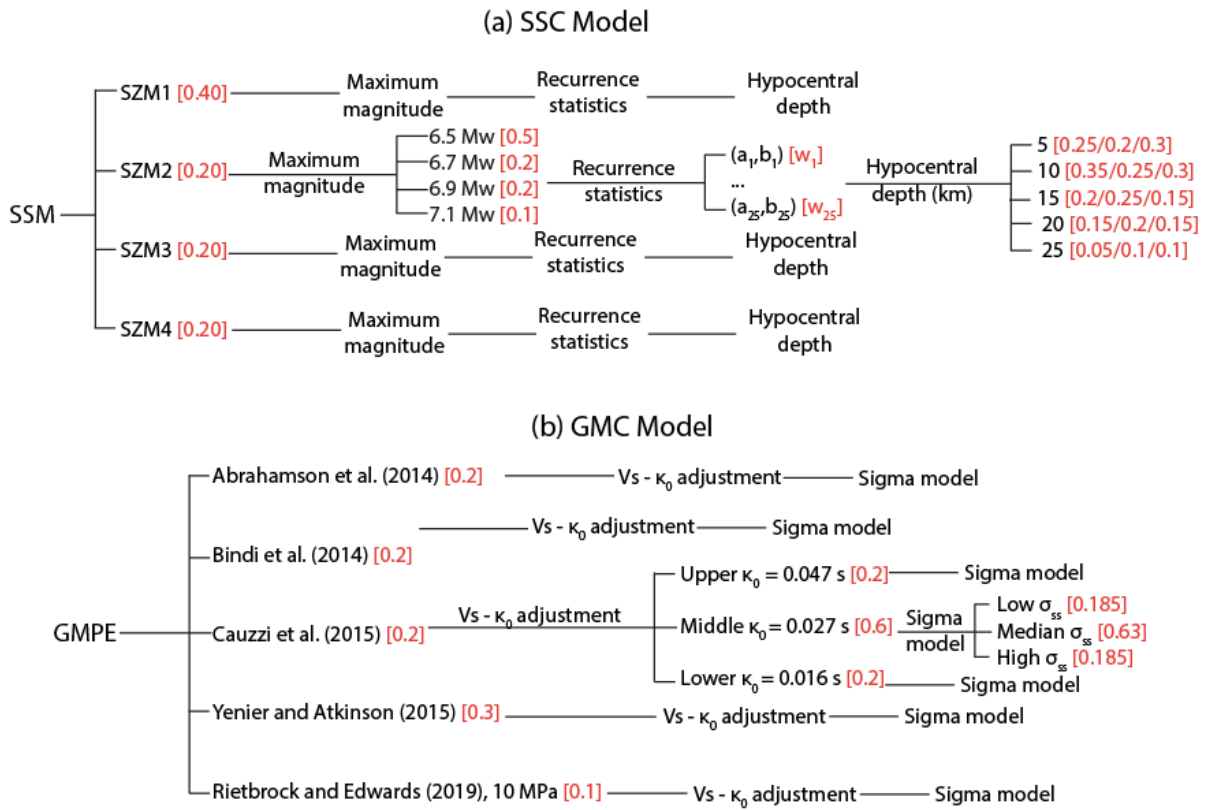


Figure 2 (a) Summary of the SSC logic tree for the 2024 offshore seismic hazard model. The three weights for the depth distribution are for the UK and Ireland, the North Sea and Northern France and Belgium. (b) Summary of the GMC logic tree for the 2024 offshore seismic hazard model. The SSC and GMC logic trees are from Mosca et al. (2024).

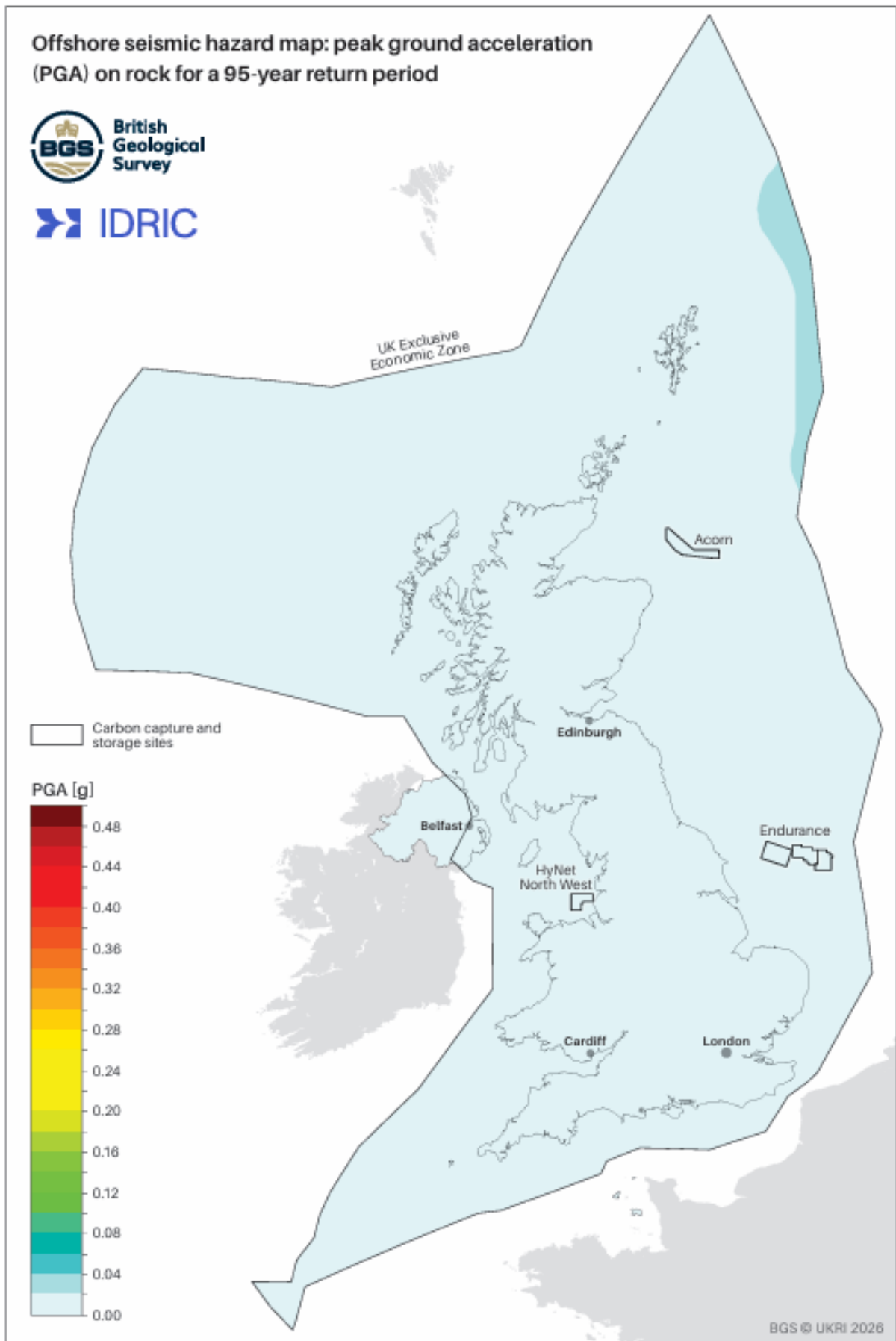


Figure 3 Hazard map for PGA for a 95-year return period. The large, black polygon describes the UK offshore EEZ. BGS © UKRI 2026. Contains OS data © Crown copyright and database right 2026.

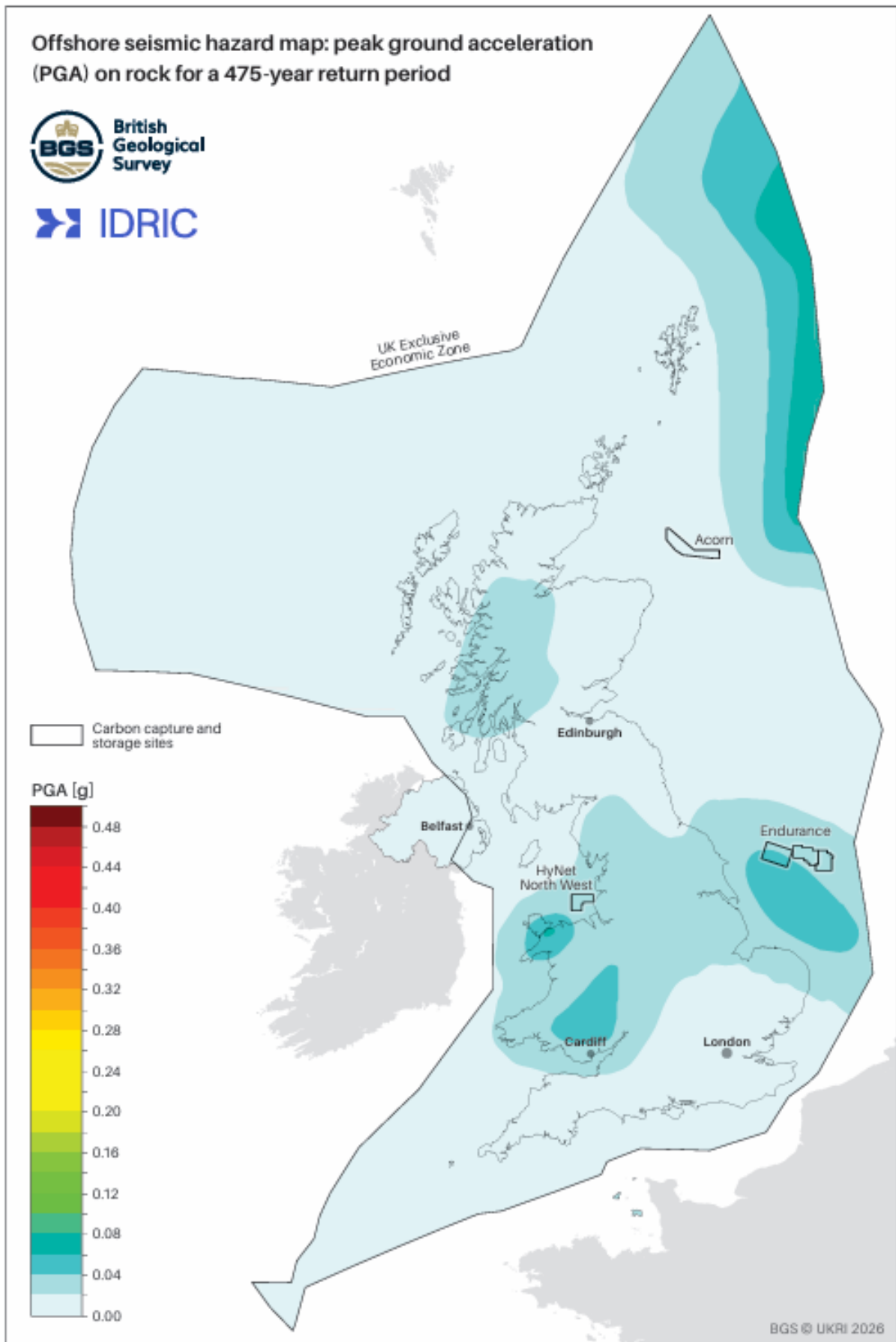


Figure 4 Hazard map for PGA for a 475-year return period. The large, black polygon describes the UK offshore EEZ. BGS © UKRI 2026. Contains OS data © Crown copyright and database right 2026.

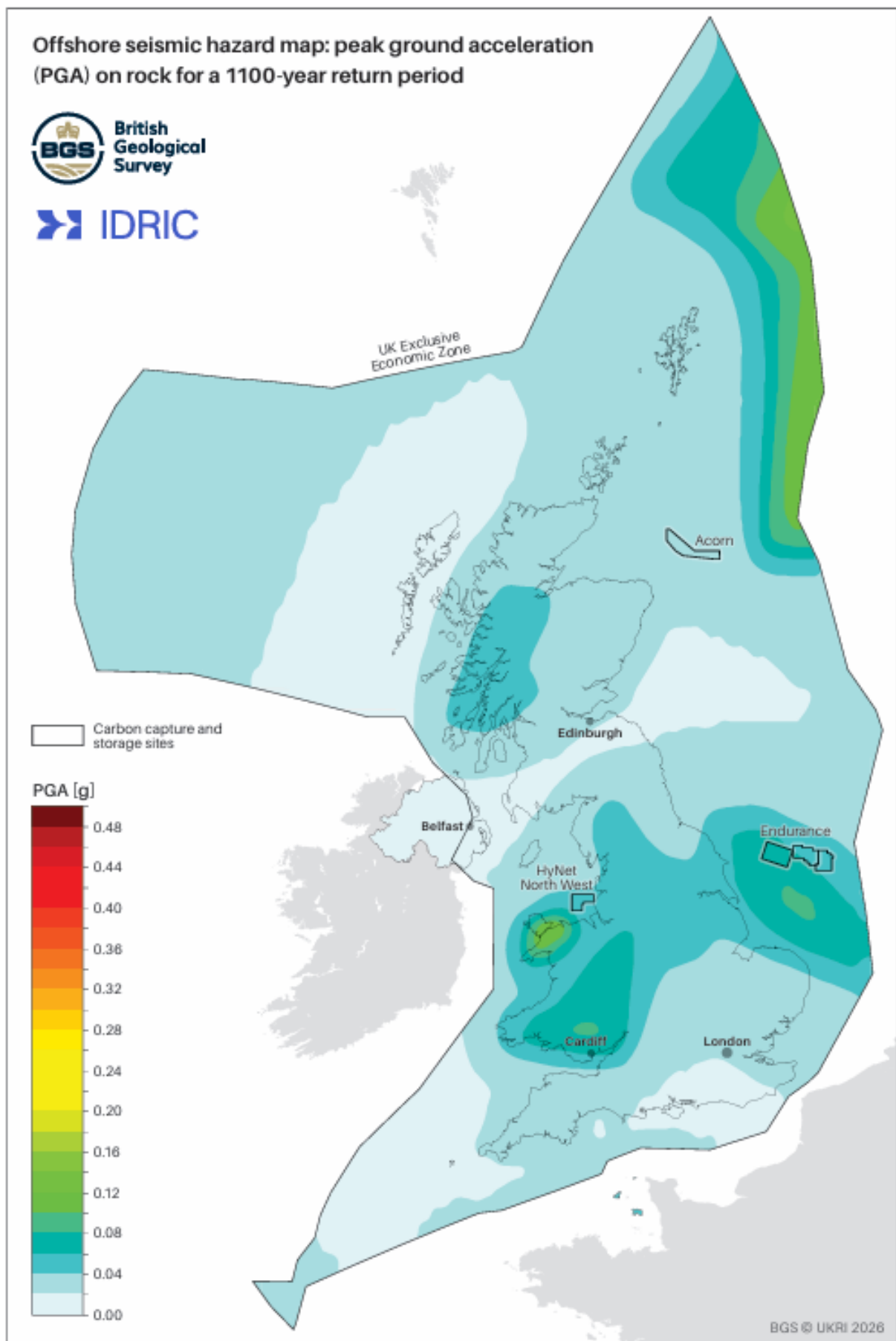


Figure 5 Hazard map for PGA for a 1100-year return period. The large, black polygon describes the UK offshore EEZ. BGS © UKRI 2026. Contains OS data © Crown copyright and database right 2026.

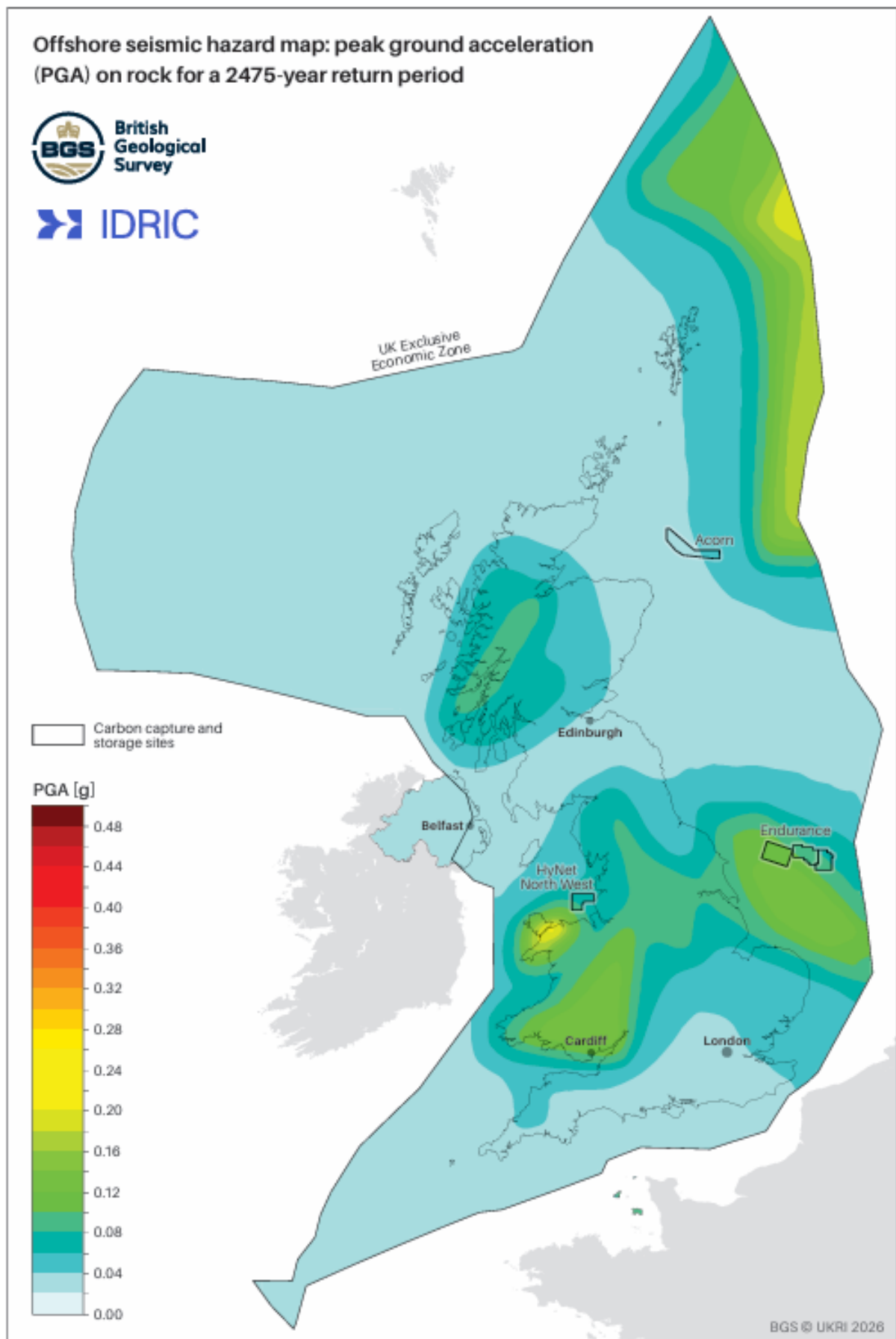


Figure 6 Hazard map for PGA for a 2475-year return period. The large, black polygon describes the UK offshore EEZ. BGS © UKRI 2026. Contains OS data © Crown copyright and database right 2026.

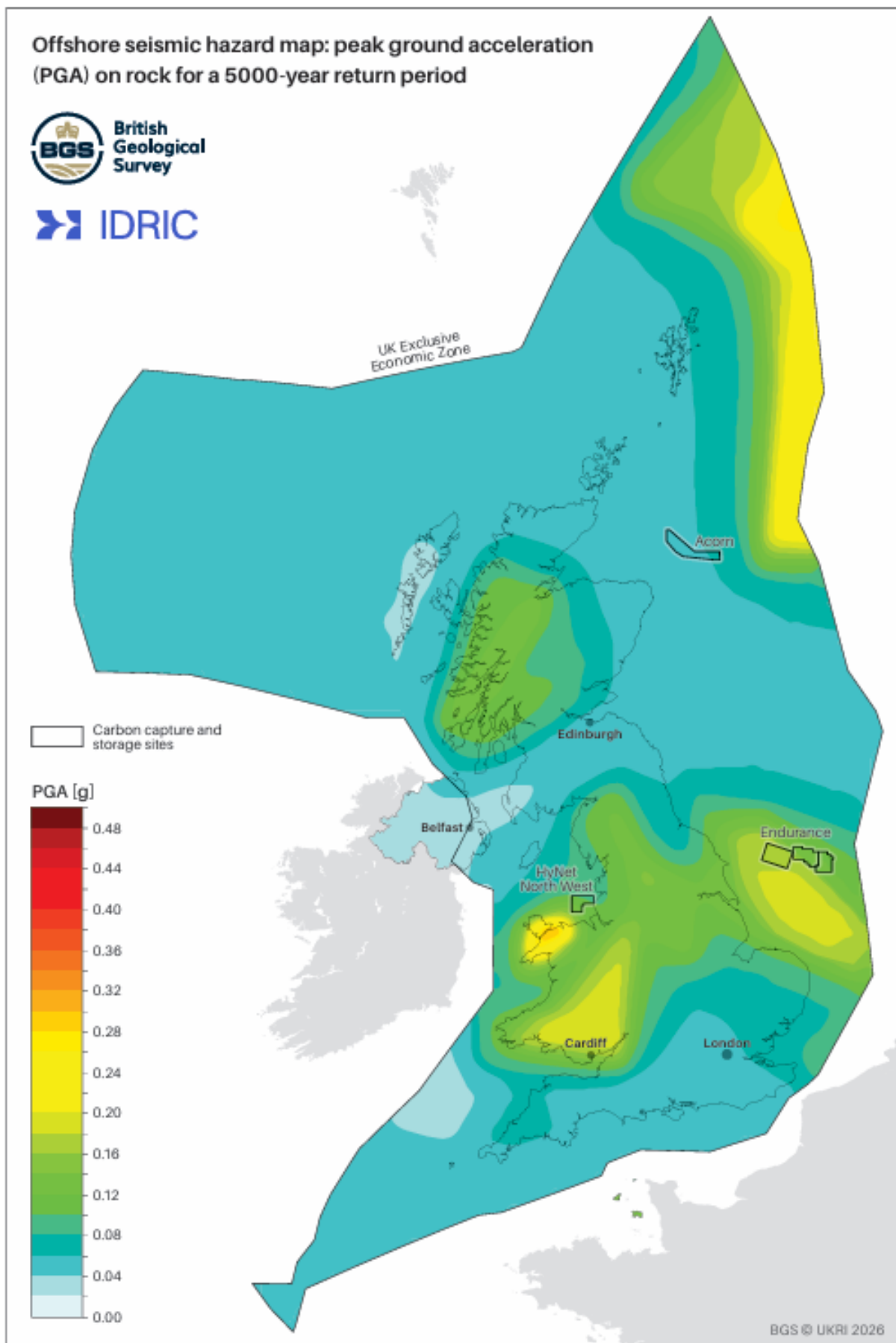


Figure 7 Hazard map for PGA for a 5000-year return period. The large, black polygon describes the UK offshore EEZ. BGS © UKRI 2026. Contains OS data © Crown copyright and database right 2026.

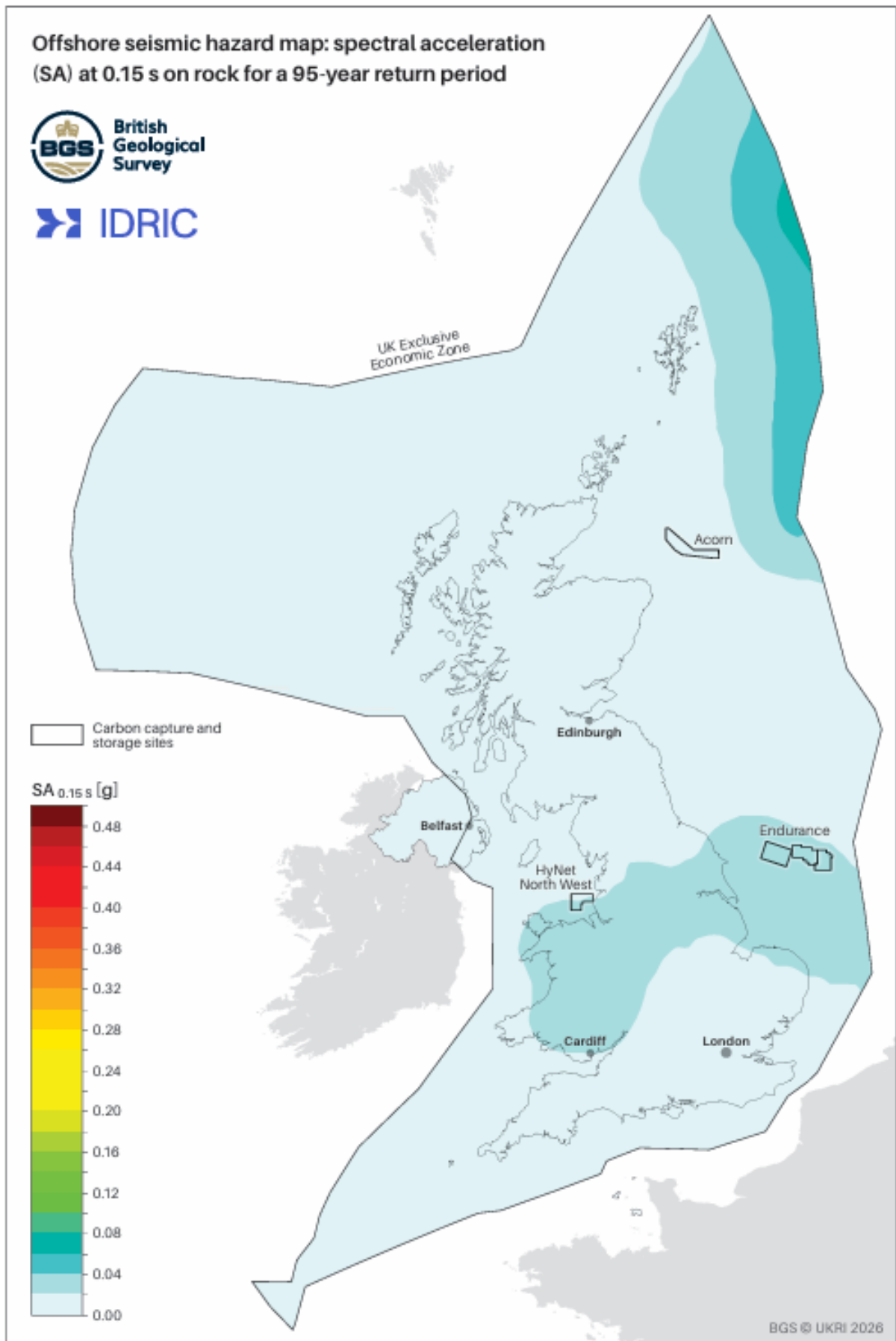


Figure 8 Hazard map for SA_{0.15 s} for a 95-year return period. The large, black polygon describes the UK offshore EEZ. BGS © UKRI 2026. Contains OS data © Crown copyright and database right 2026.

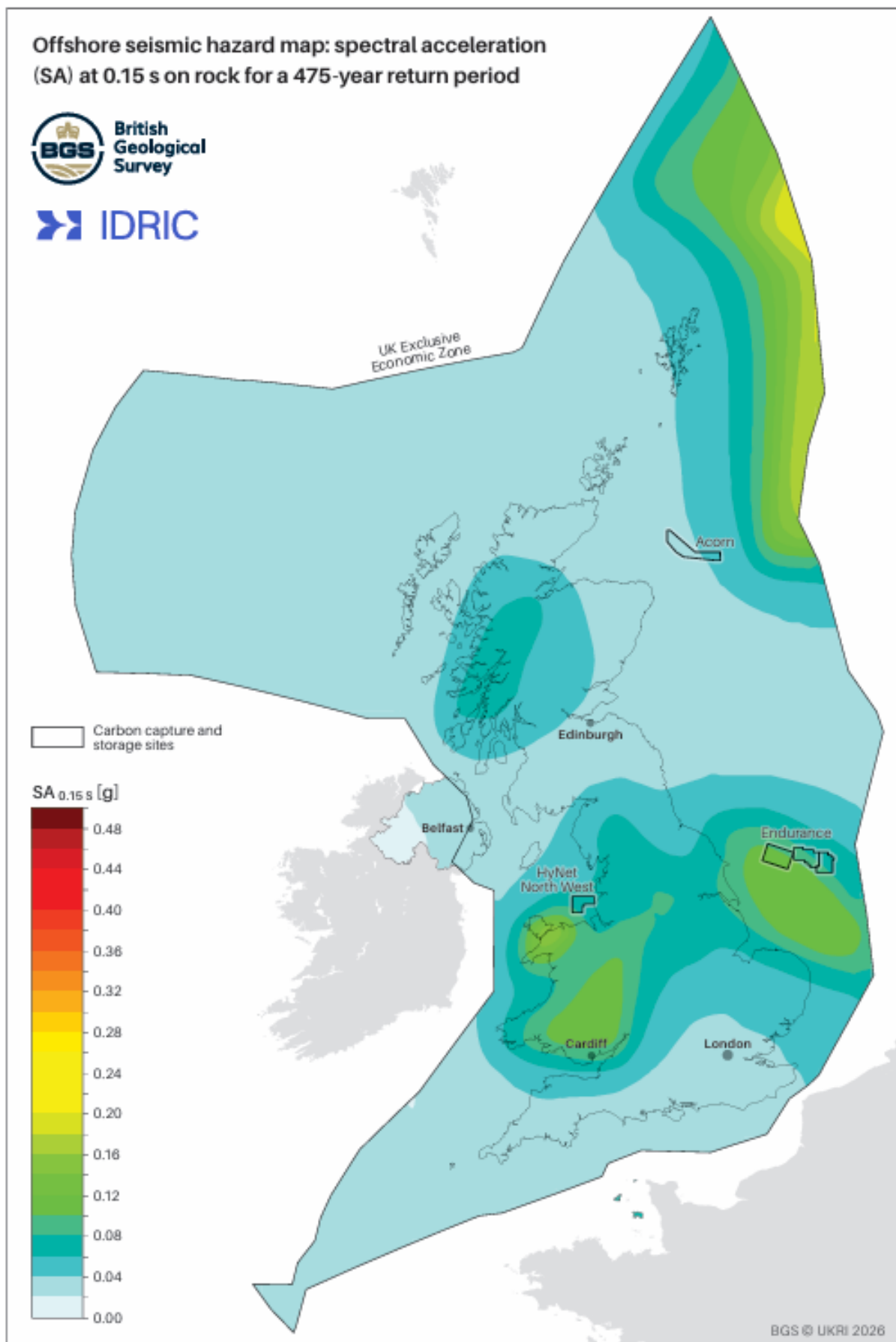


Figure 9 Hazard map for SA_{0.15 s} for a 475-year return period. The large, black polygon describes the UK offshore EEZ. BGS © UKRI 2026. Contains OS data © Crown copyright and database right 2026.

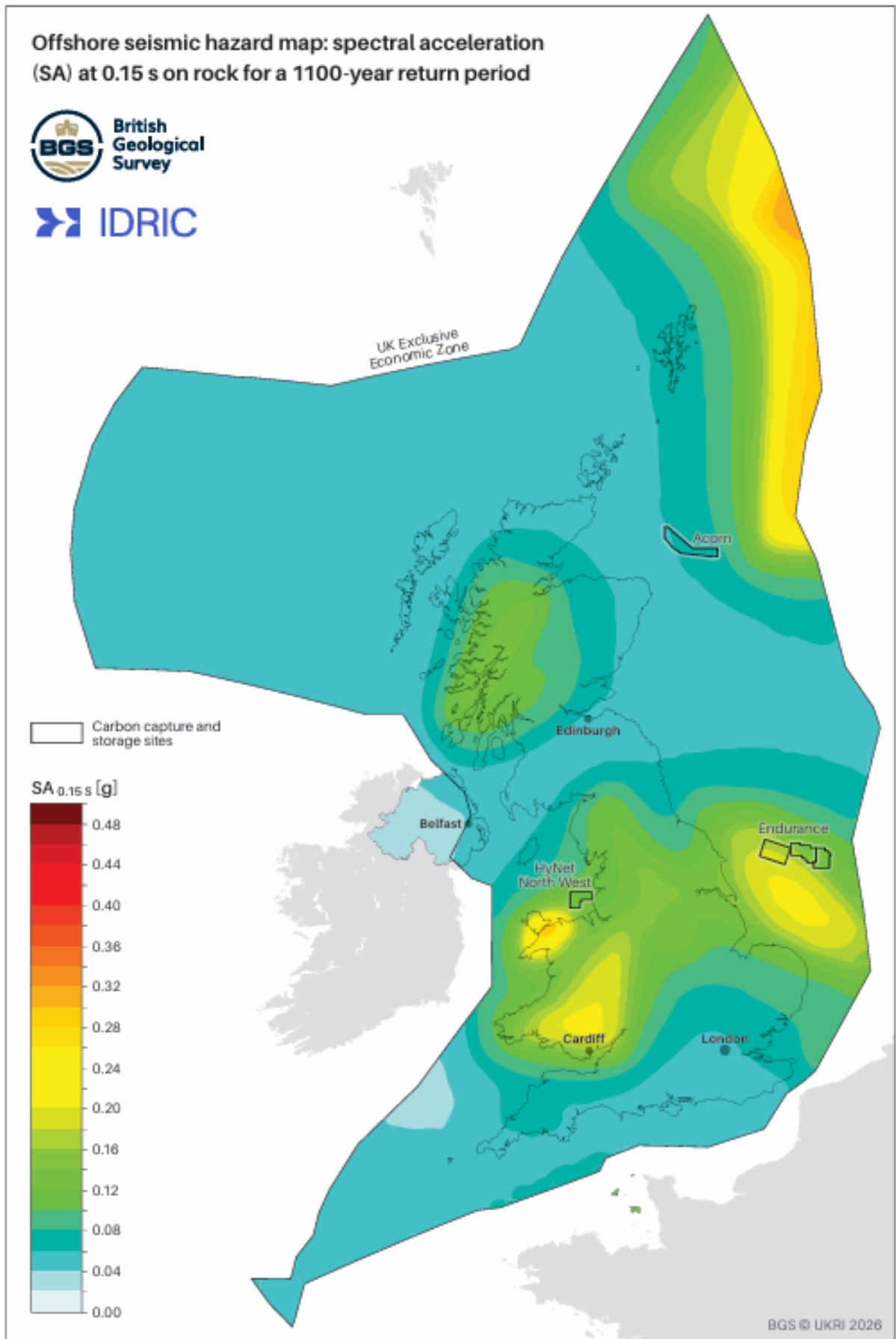


Figure 10 Hazard map for SA_{0.15 s} for a 1100-year return period. The large, black polygon describes the UK offshore EEZ. BGS © UKRI 2026. Contains OS data © Crown copyright and database right 2026.

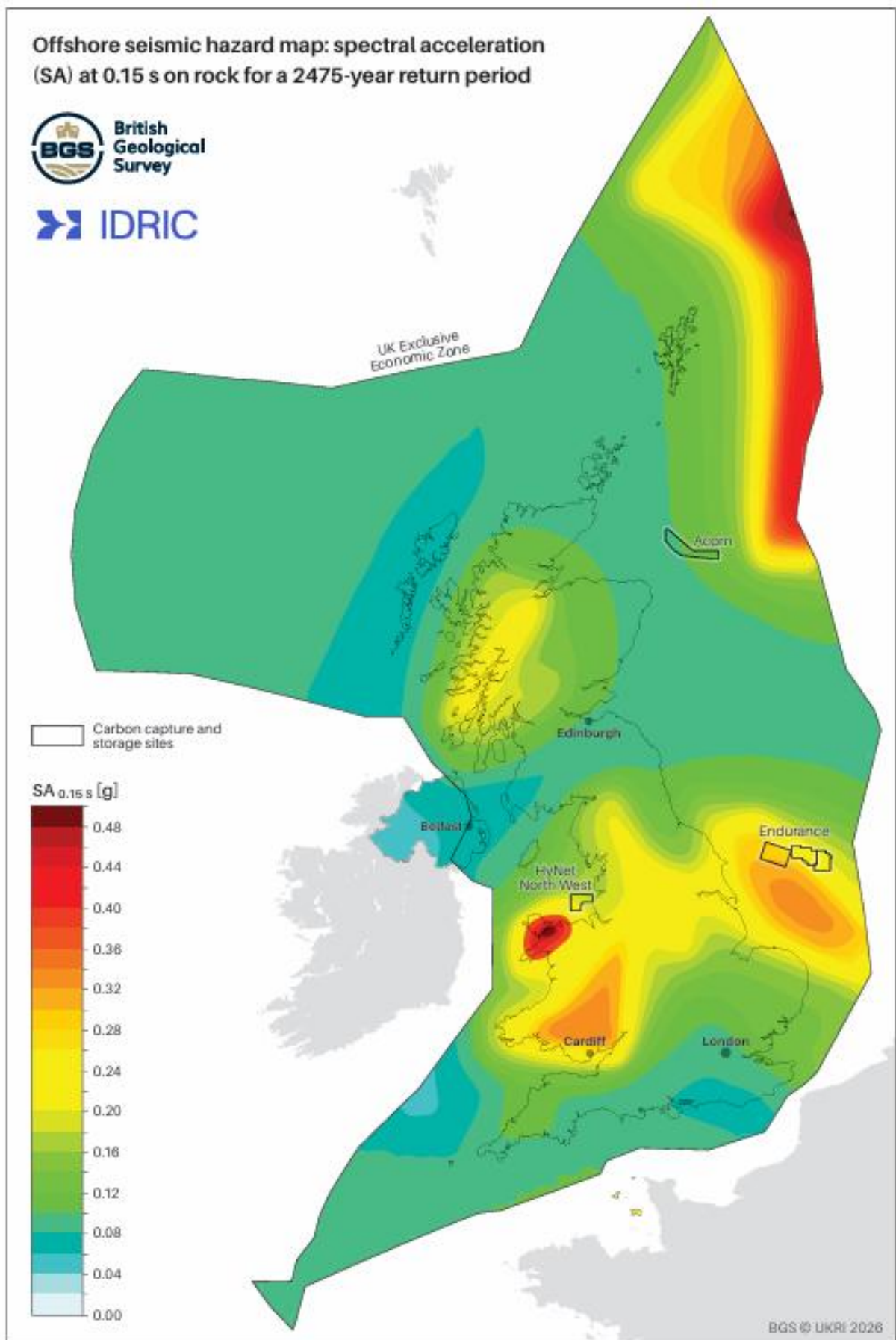


Figure 11 Hazard map for SA_{0.15 s} for a 2475-year return period. The large, black polygon describes the UK offshore EEZ. BGS © UKRI 2026. Contains OS data © Crown copyright and database right 2026.

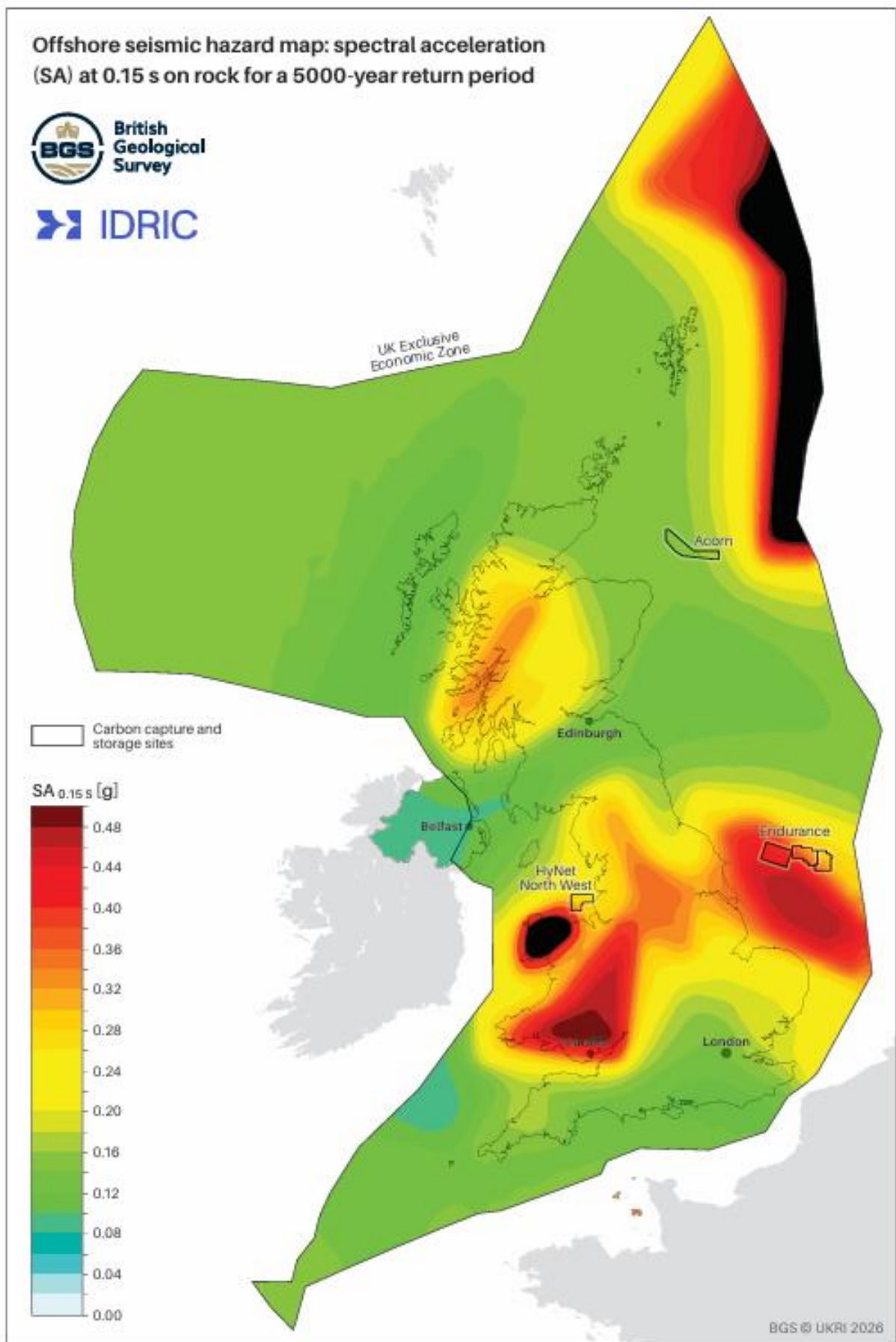


Figure 12 Hazard map for SA_{0.15 s} for a 5000-year return period. The large, black polygon describes the UK offshore EEZ. BGS © UKRI 2026. Contains OS data © Crown copyright and database right 2026.

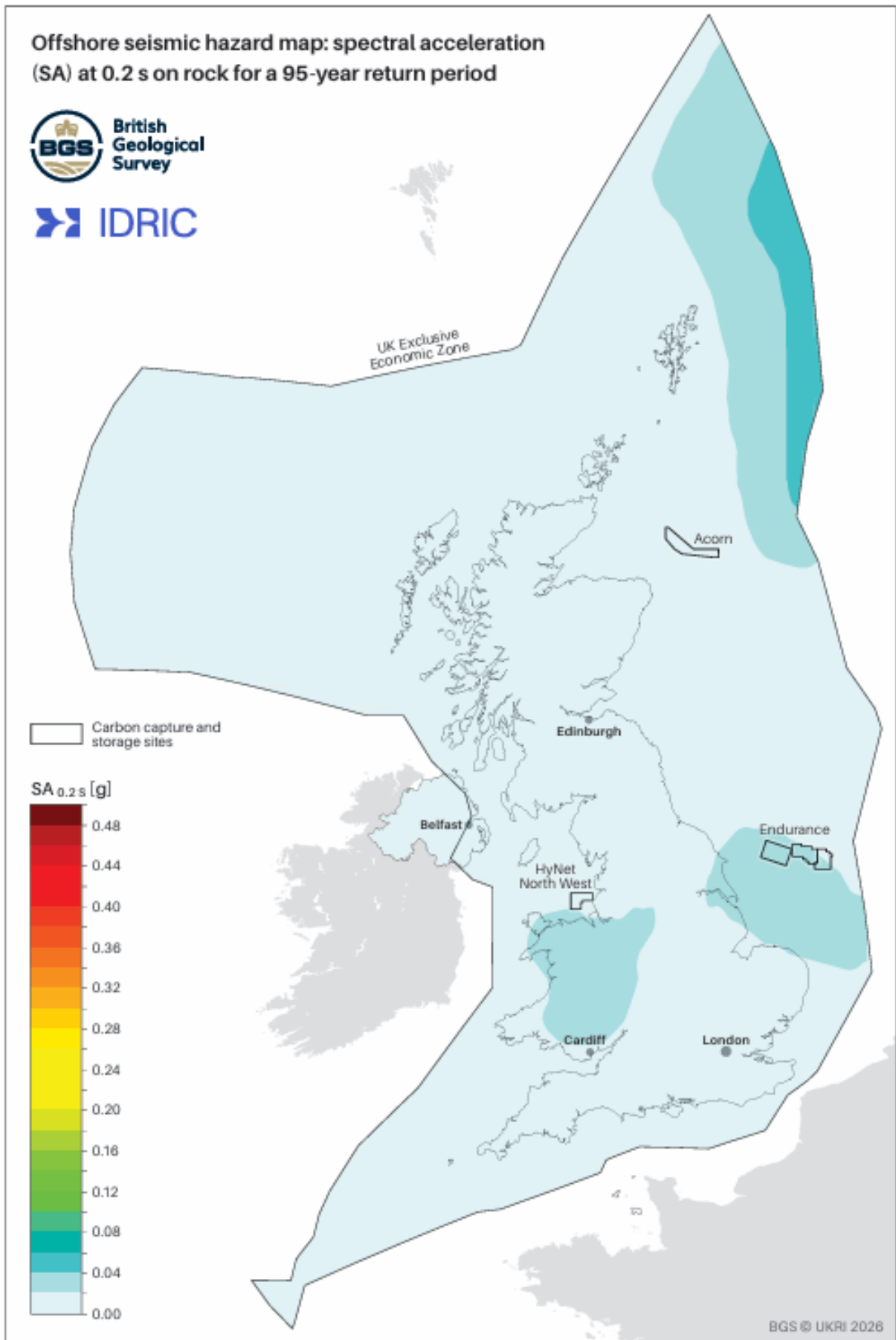


Figure 13 Hazard map for SA_{0.20 s} for a 95-year return period. The large, black polygon describes the UK offshore EEZ. BGS © UKRI 2026. Contains OS data © Crown copyright and database right 2026.

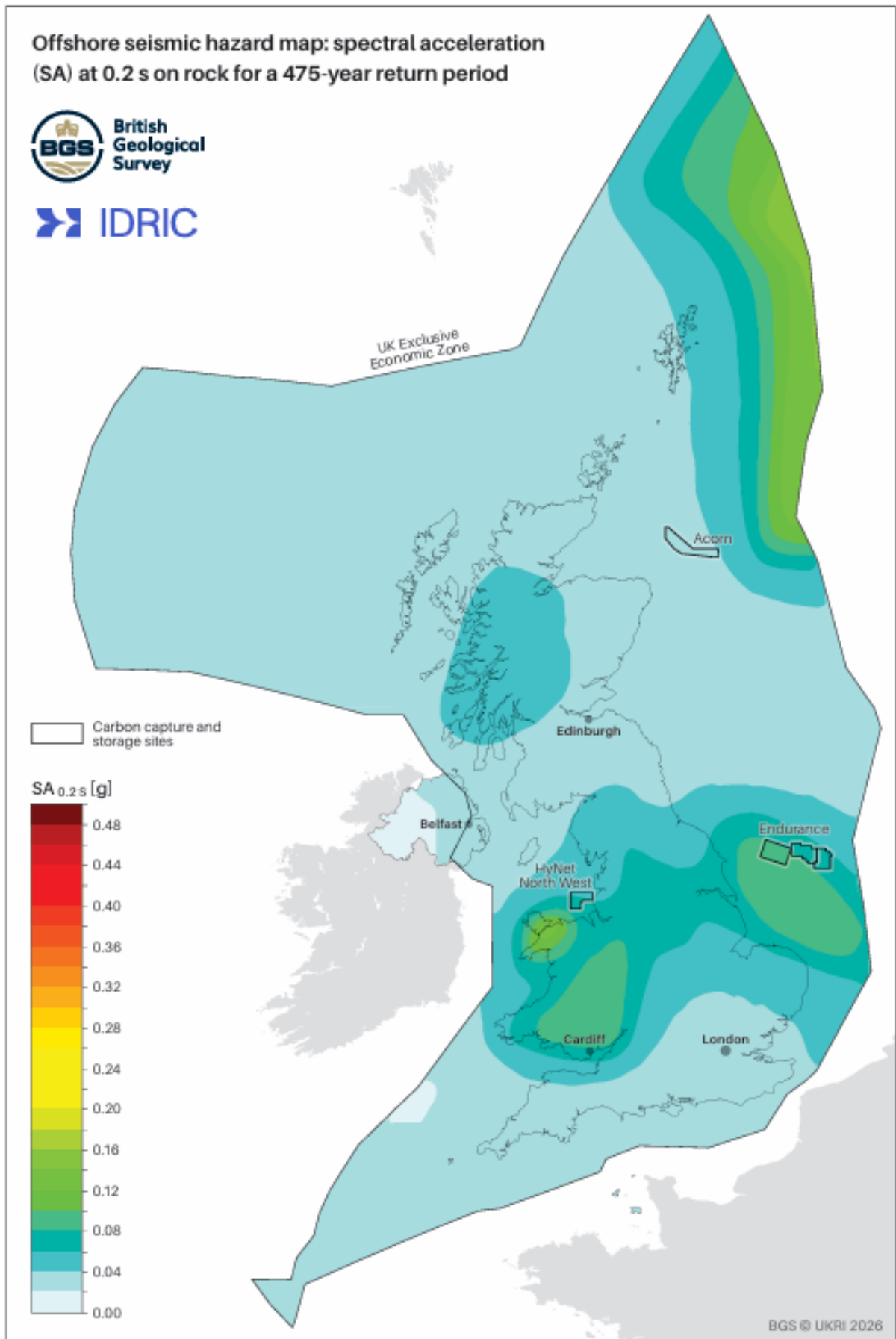


Figure 14 Hazard map for SA_{0.20s} for a 475-year return period. The large, black polygon describes the UK offshore EEZ. BGS © UKRI 2026. Contains OS data © Crown copyright and database right 2026.

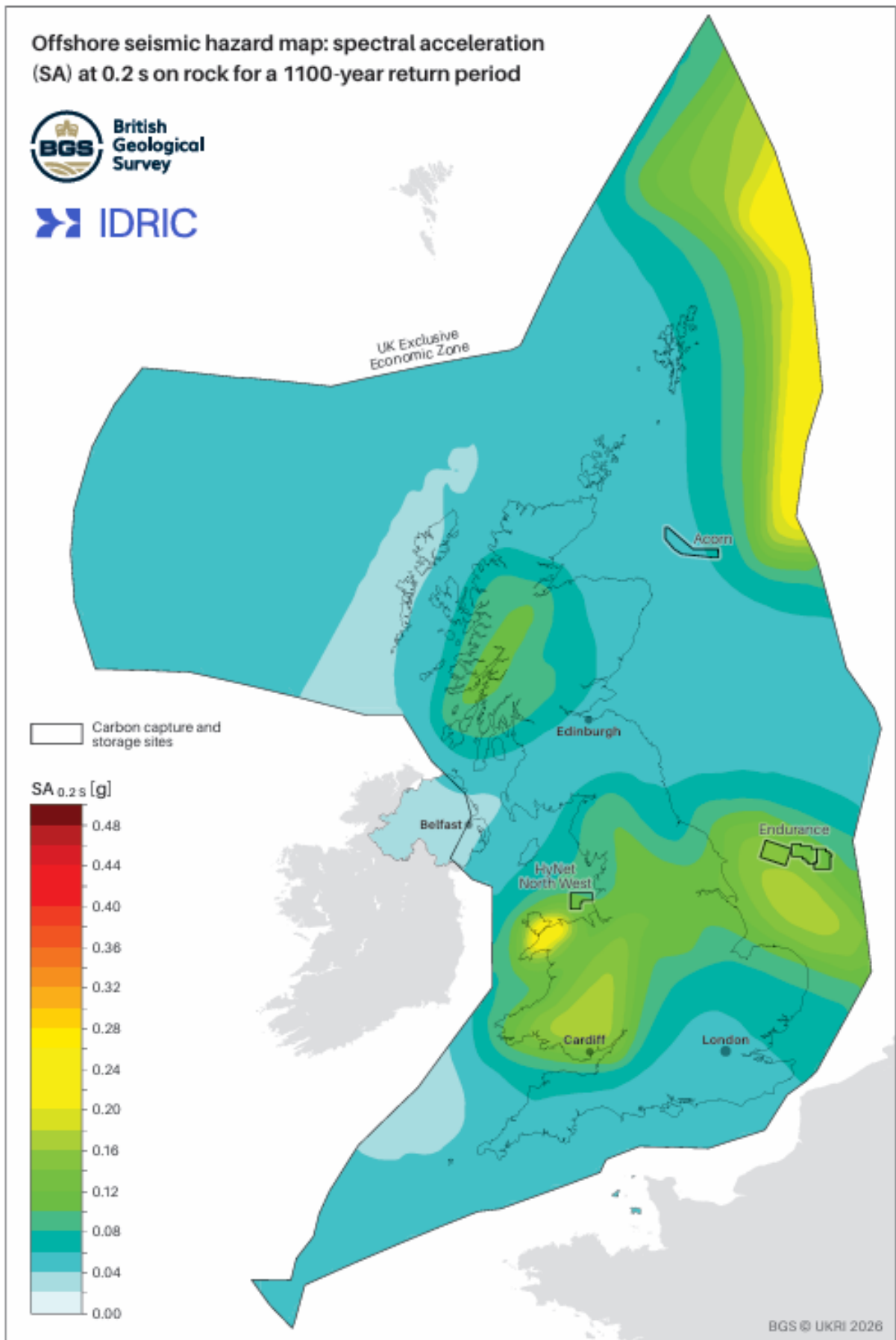


Figure 15 Hazard map for SA_{0.2s} for a 1100-year return period. The large, black polygon describes the UK offshore EEZ. BGS © UKRI 2026. Contains OS data © Crown copyright and database right 2026.

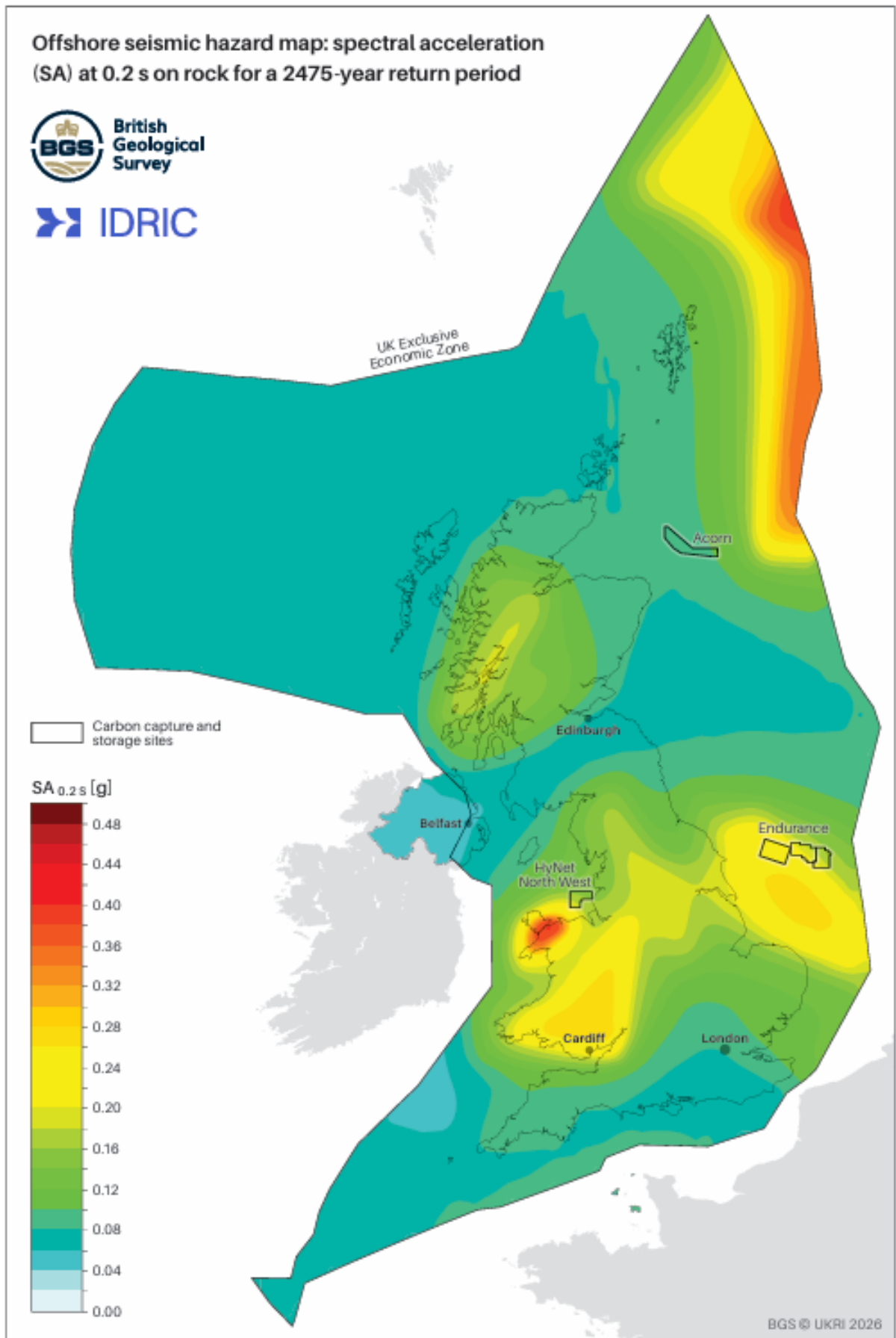


Figure 16 Hazard map for SA_{0.2s} for a 2475-year return period. The large, black polygon describes the UK offshore EEZ. BGS © UKRI 2026. Contains OS data © Crown copyright and database right 2026.

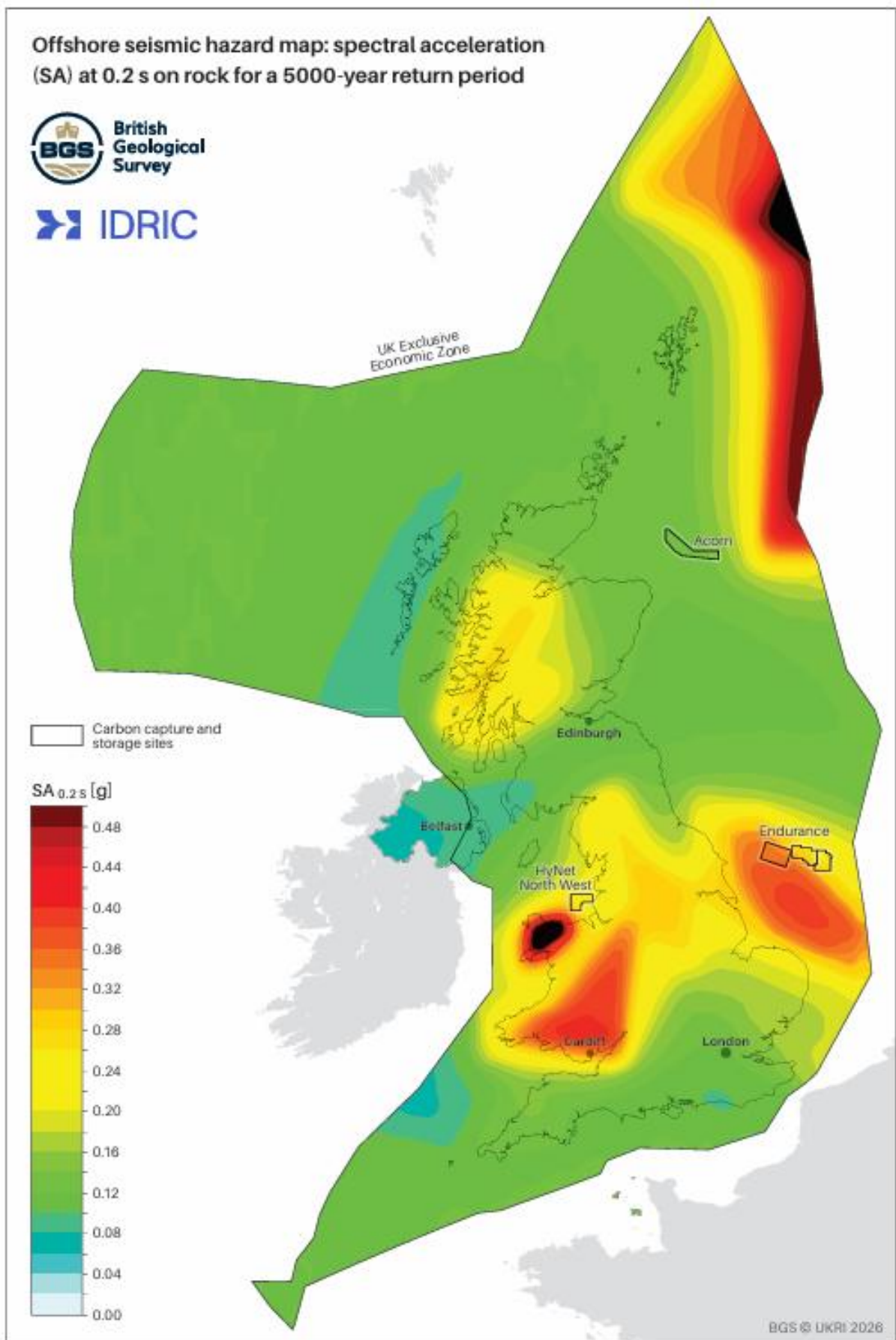


Figure 17 Hazard map for SA_{0.2s} for a 5000-year return period. The large, black polygon describes the UK offshore EEZ. BGS © UKRI 2026. Contains OS data © Crown copyright and database right 2026.

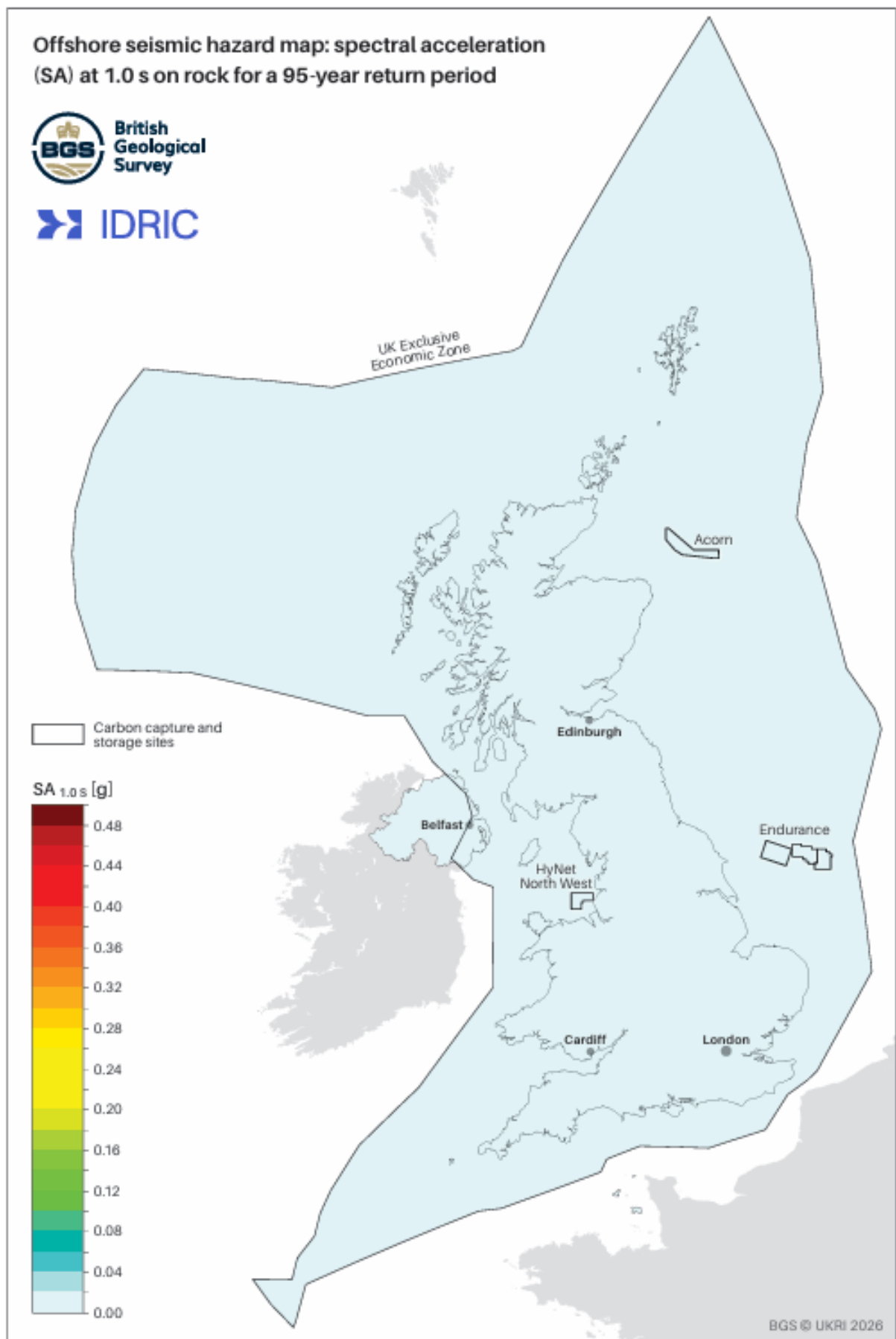


Figure 18 Hazard map for SA_{1.0 s} for a 95-year return period. The large, black polygon describes the UK offshore EEZ. BGS © UKRI 2026. Contains OS data © Crown copyright and database right 2026.

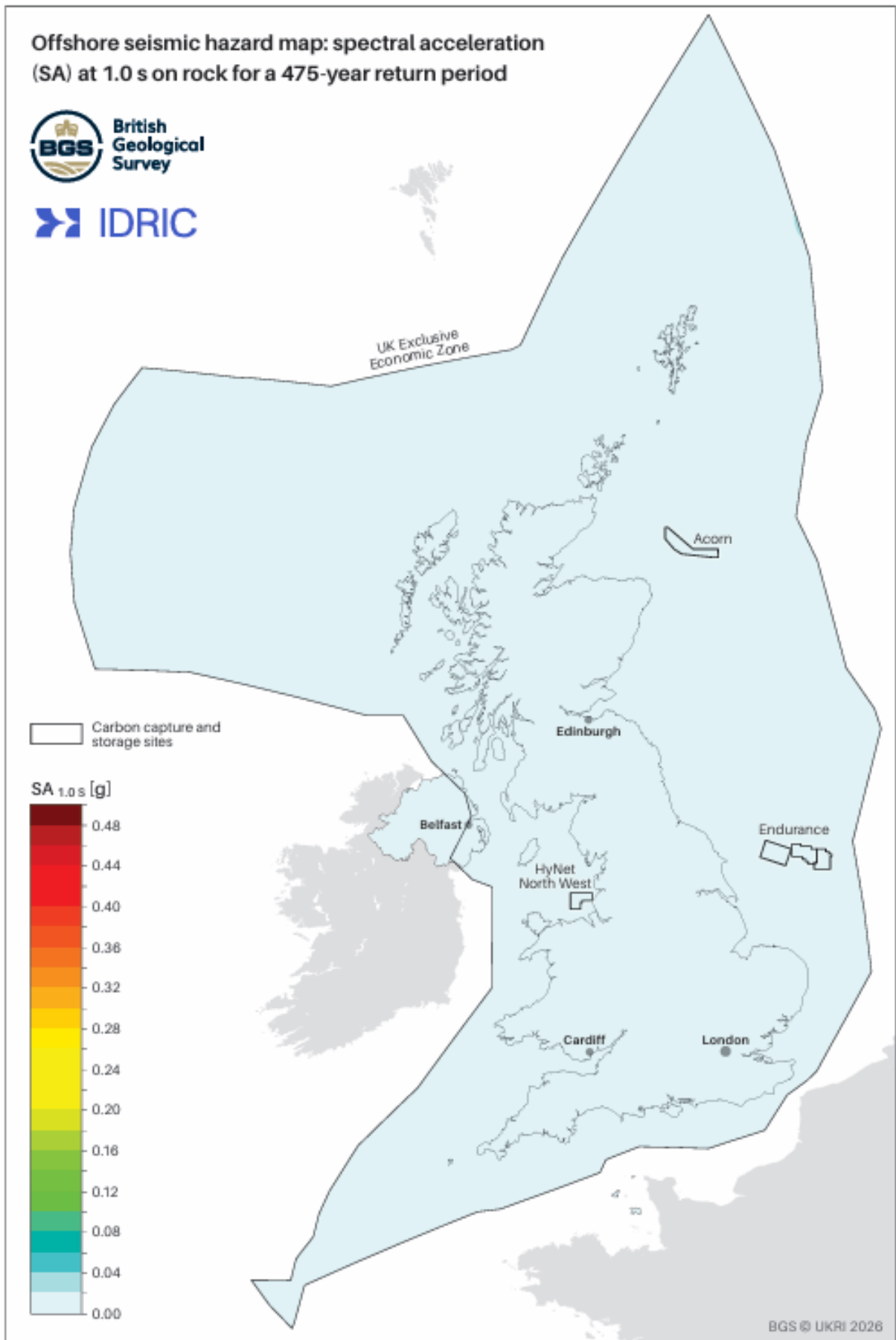


Figure 19 Hazard map for SA_{1.00s} for a 475-year return period. The large, black polygon describes the UK offshore EEZ. BGS © UKRI 2026. Contains OS data © Crown copyright and database right 2026.

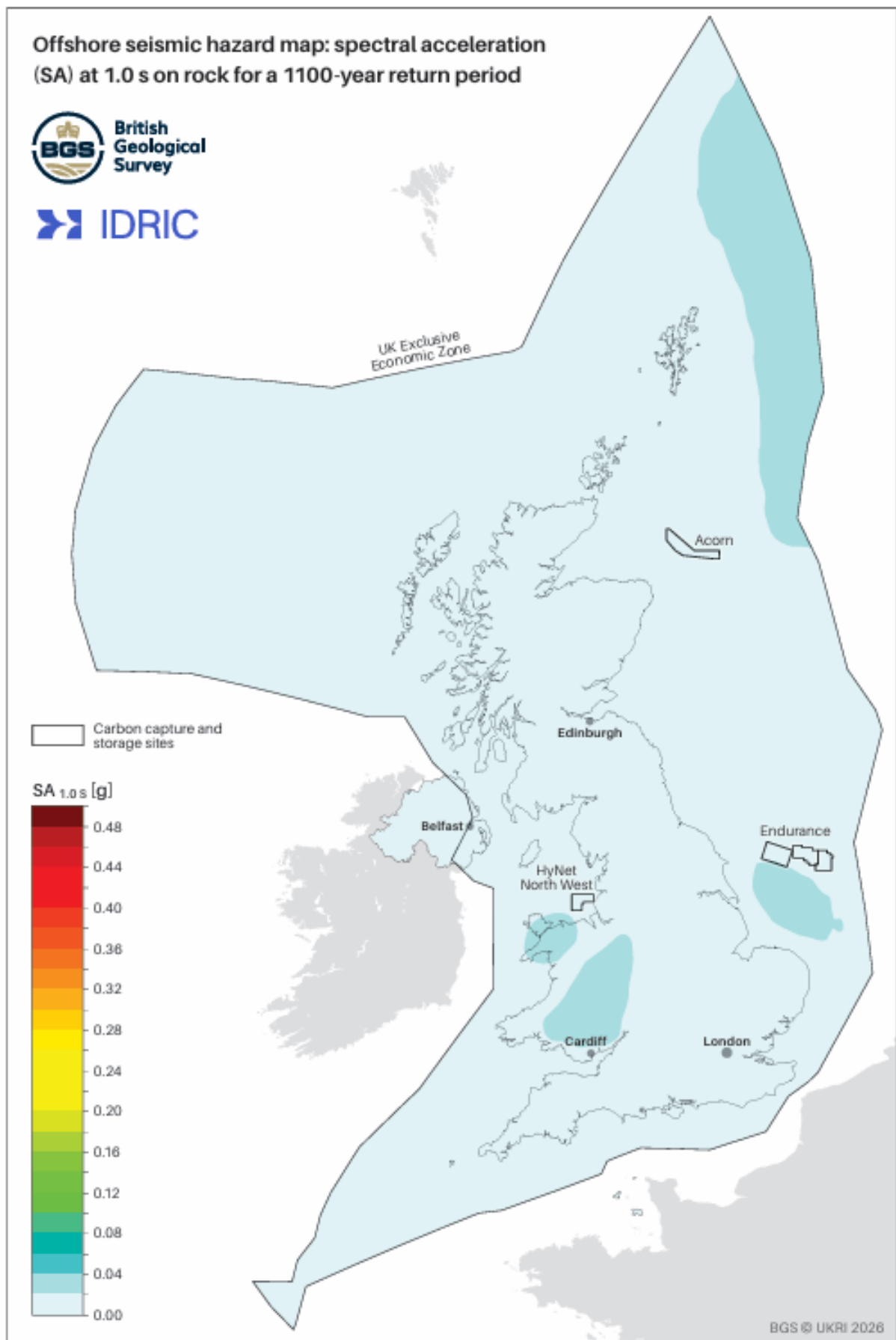


Figure 20 Hazard map for SA_{1.0s} for a 1100-year return period. The large, black polygon describes the UK offshore EEZ. BGS © UKRI 2026. Contains OS data © Crown copyright and database right 2026.

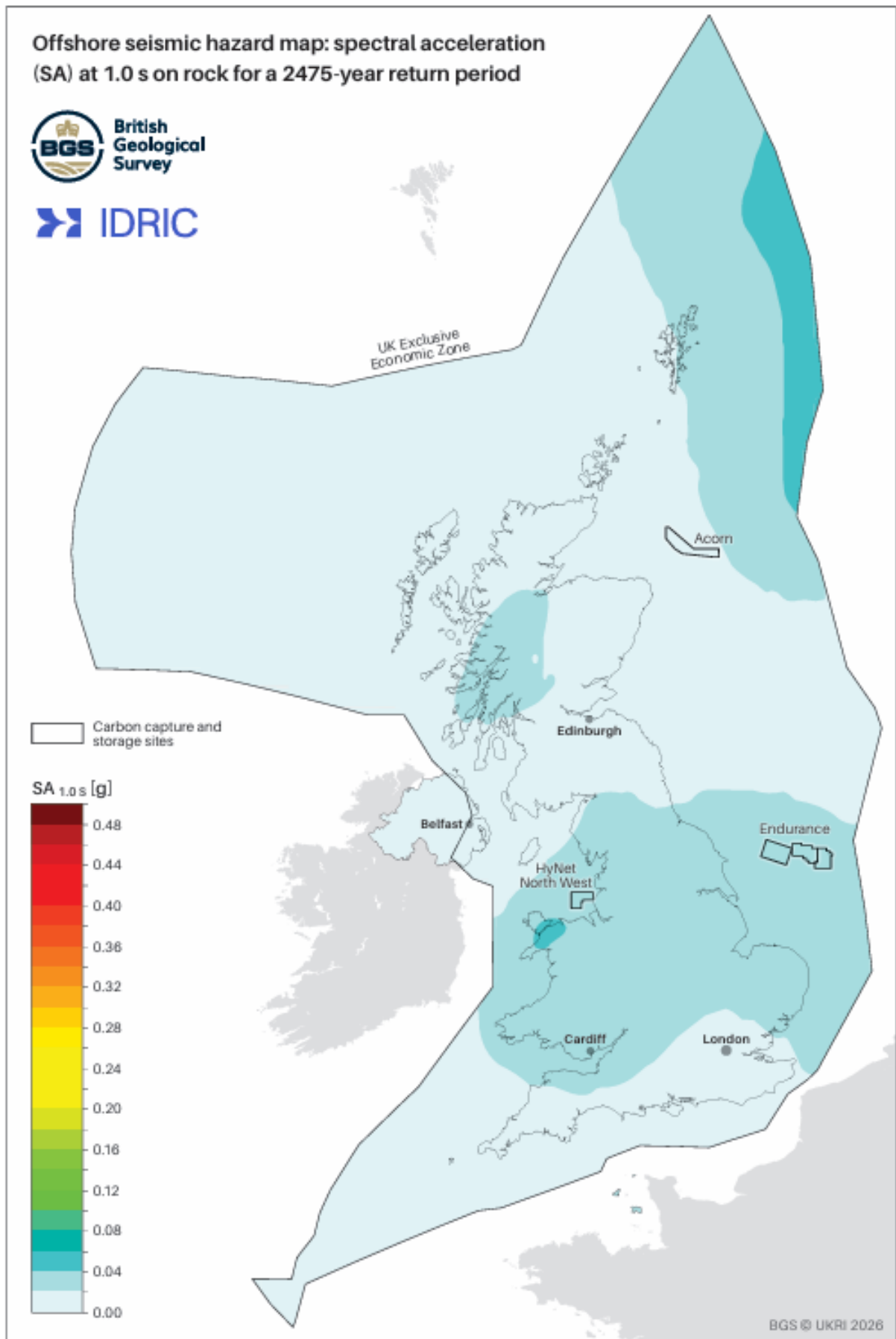


Figure 21 Hazard map for SA_{1.0s} for a 2475-year return period. The large, black polygon describes the UK offshore EEZ. BGS © UKRI 2026. Contains OS data © Crown copyright and database right 2026.

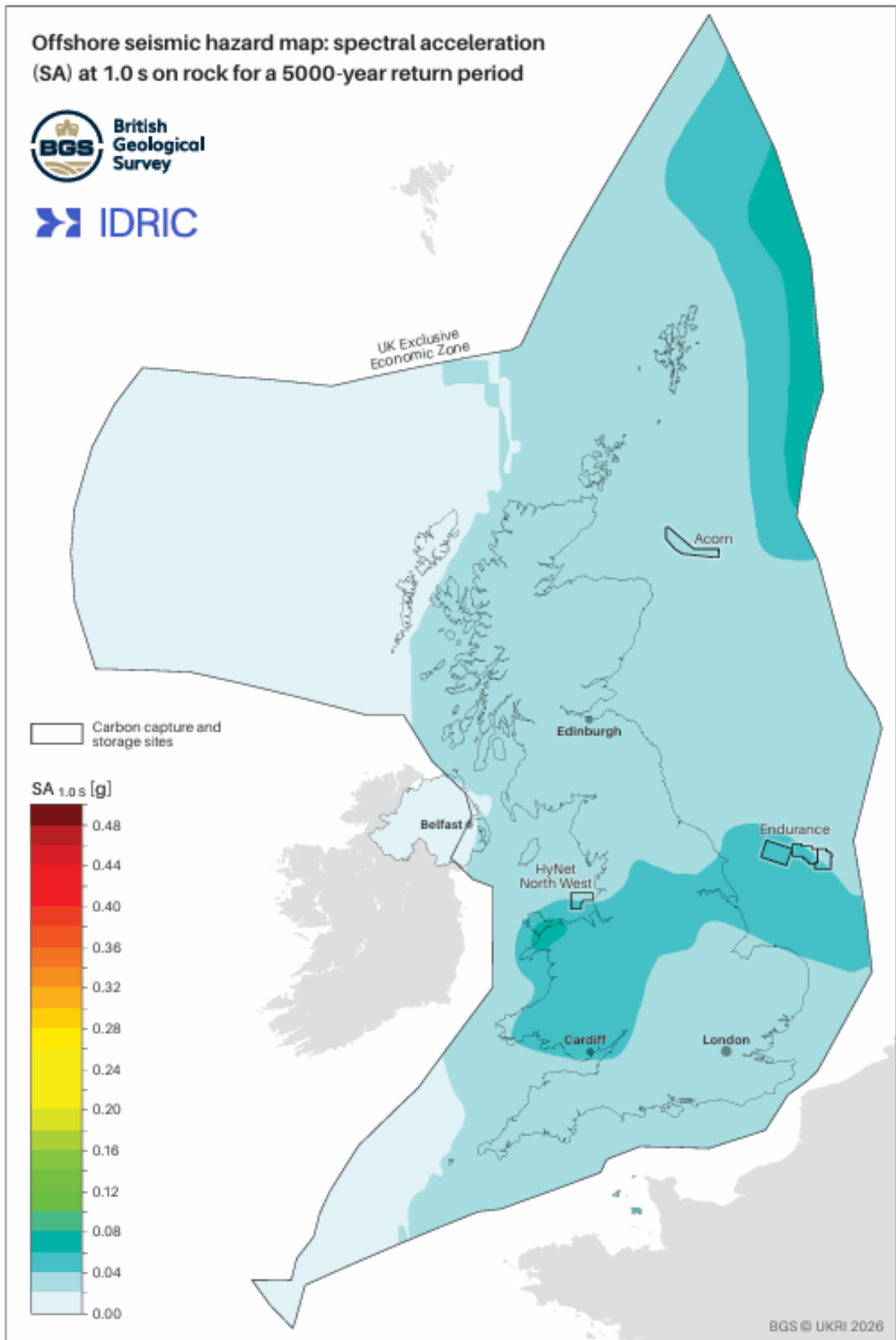


Figure 22 Hazard map for SA_{1.0s} for a 5000-year return period. The large, black polygon describes the UK offshore EEZ. BGS © UKRI 2026. Contains OS data © Crown copyright and database right 2026.

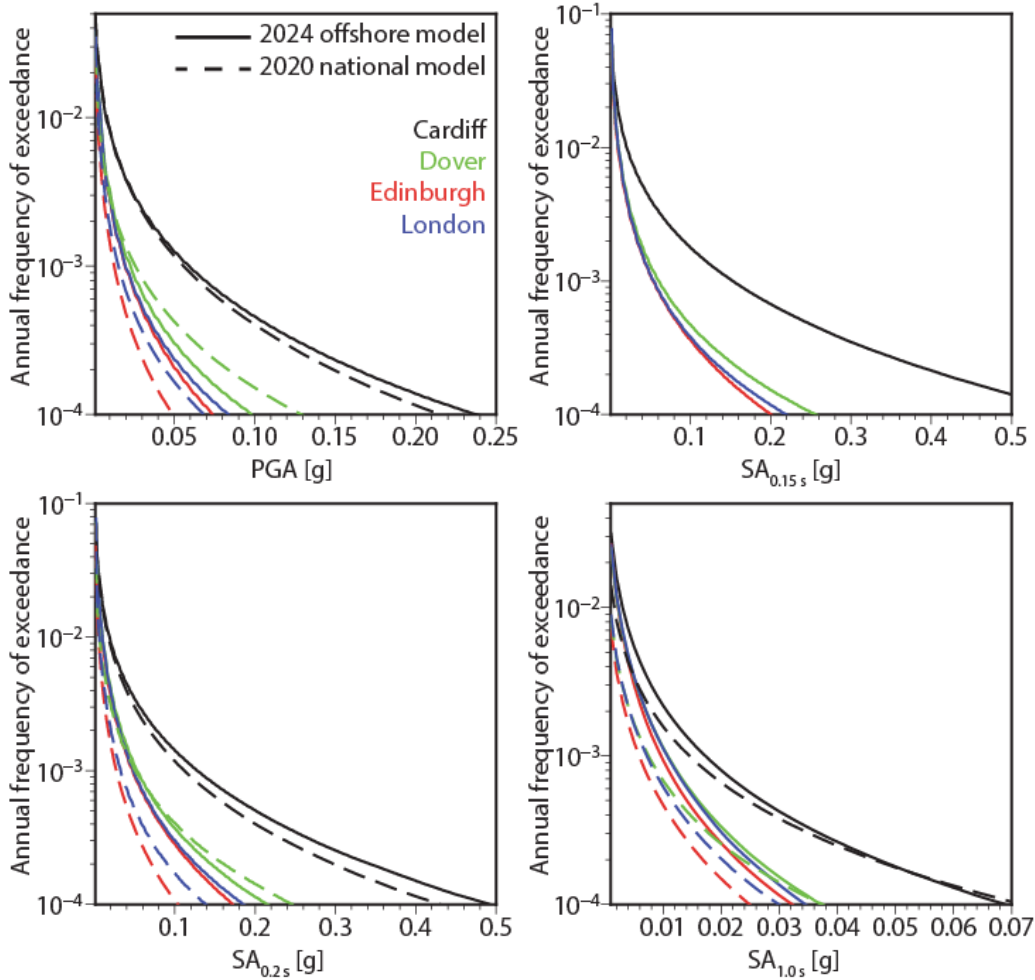


Figure 23 PGA, $SA_{0.15s}$, $SA_{0.25s}$, and $SA_{1.00s}$ hazard curves for sites in Cardiff, Dover, Edinburgh, and London. Solid and dashed lines are the hazard curves computed using the 2024 offshore hazard model and the 2020 national hazard model, respectively.

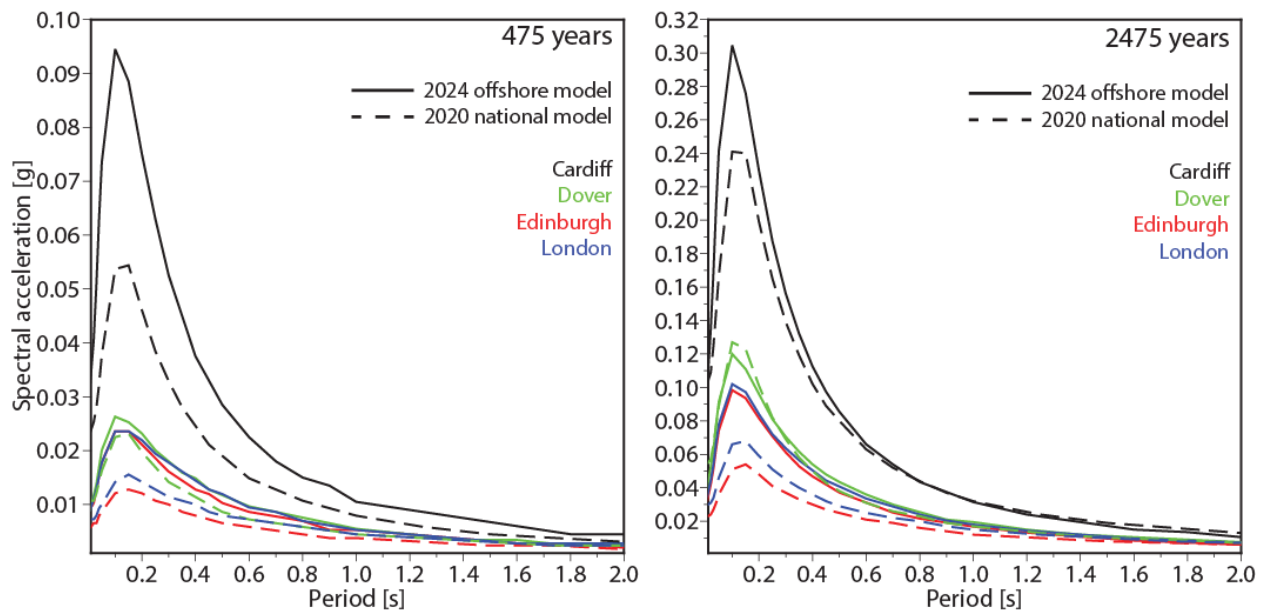


Figure 24 UHS for return periods of 475 years and 2475 years for sites in Cardiff, Dover, Edinburgh, and London. Solid and dashed lines are computed using the 2024 offshore hazard model and the 2020 national hazard model, respectively.

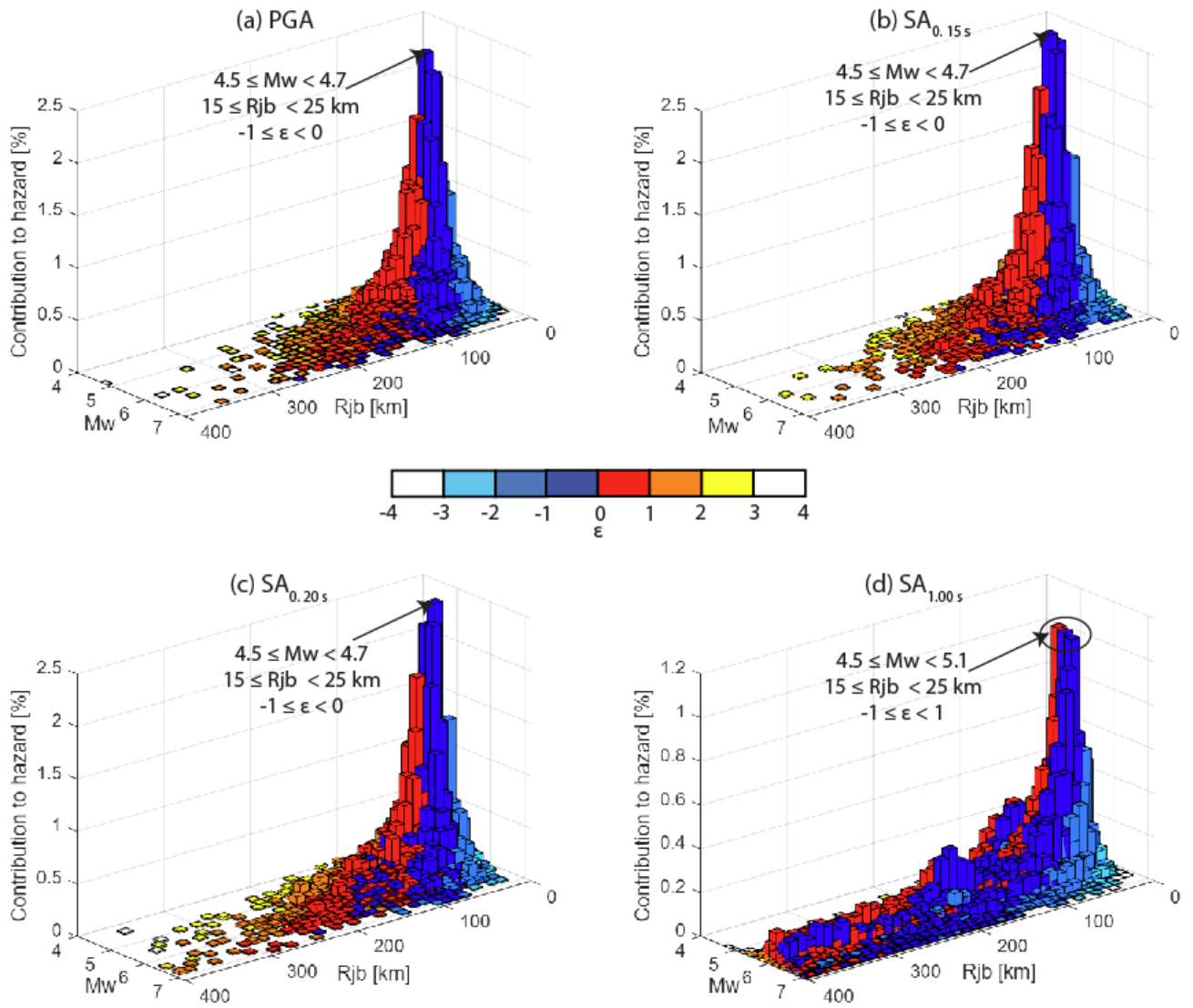


Figure 25 Disaggregation of the hazard for the Cardiff site and 475-year return period by magnitude (Mw), Joyner-Boore distance (Rjb) and epsilon (ϵ) for (a) PGA, (b) $SA_{0.2s}$, (c) $SA_{0.2s}$, and (d) $SA_{1.0s}$.

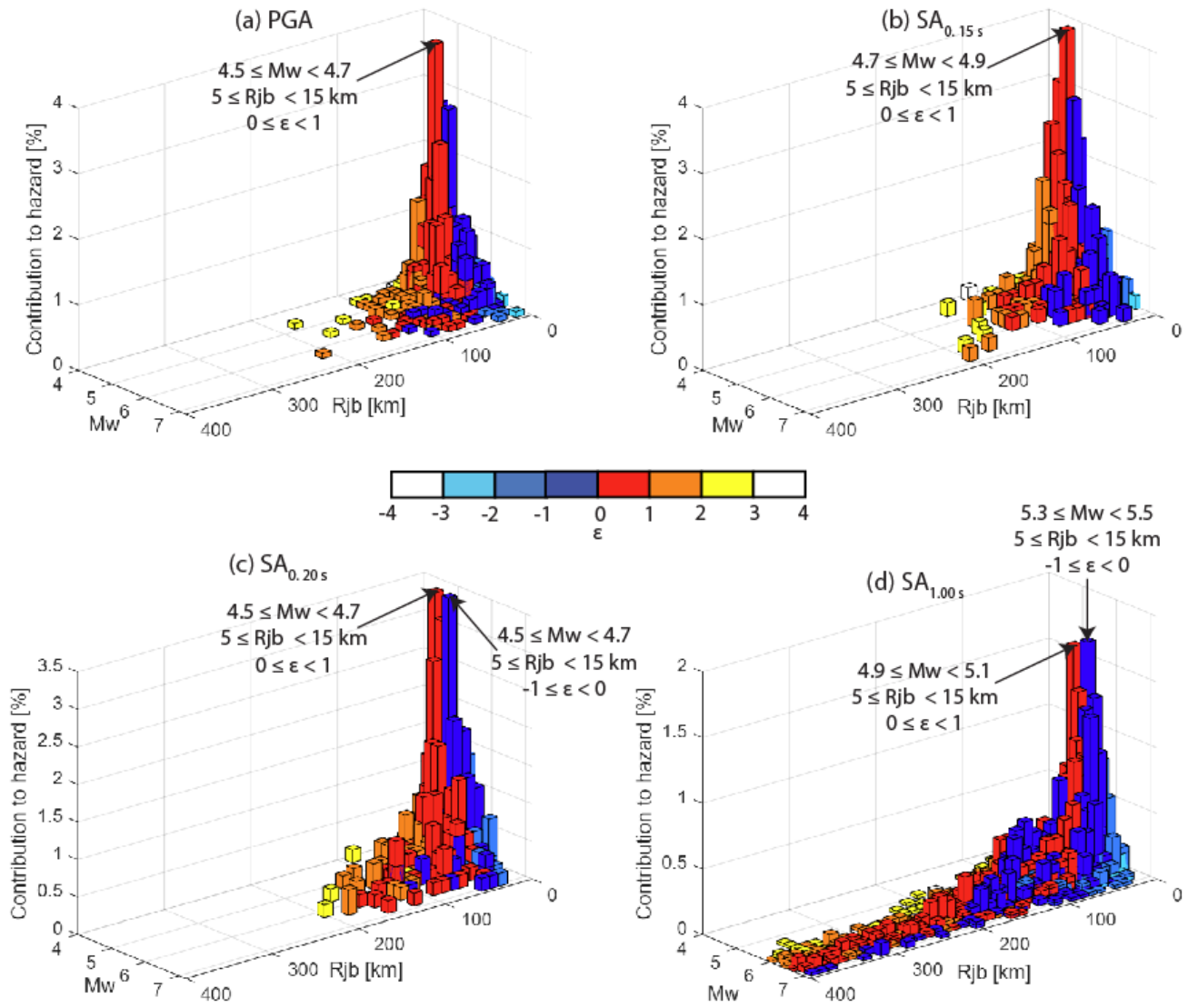


Figure 26 Disaggregation of the hazard for the Cardiff site and 2475-year return period by magnitude (Mw), Joyner-Boore distance (Rjb) and epsilon (ϵ) for (a) PGA, (b) $SA_{0.2s}$, (c) $SA_{0.2s}$, and (d) $SA_{1.0s}$.

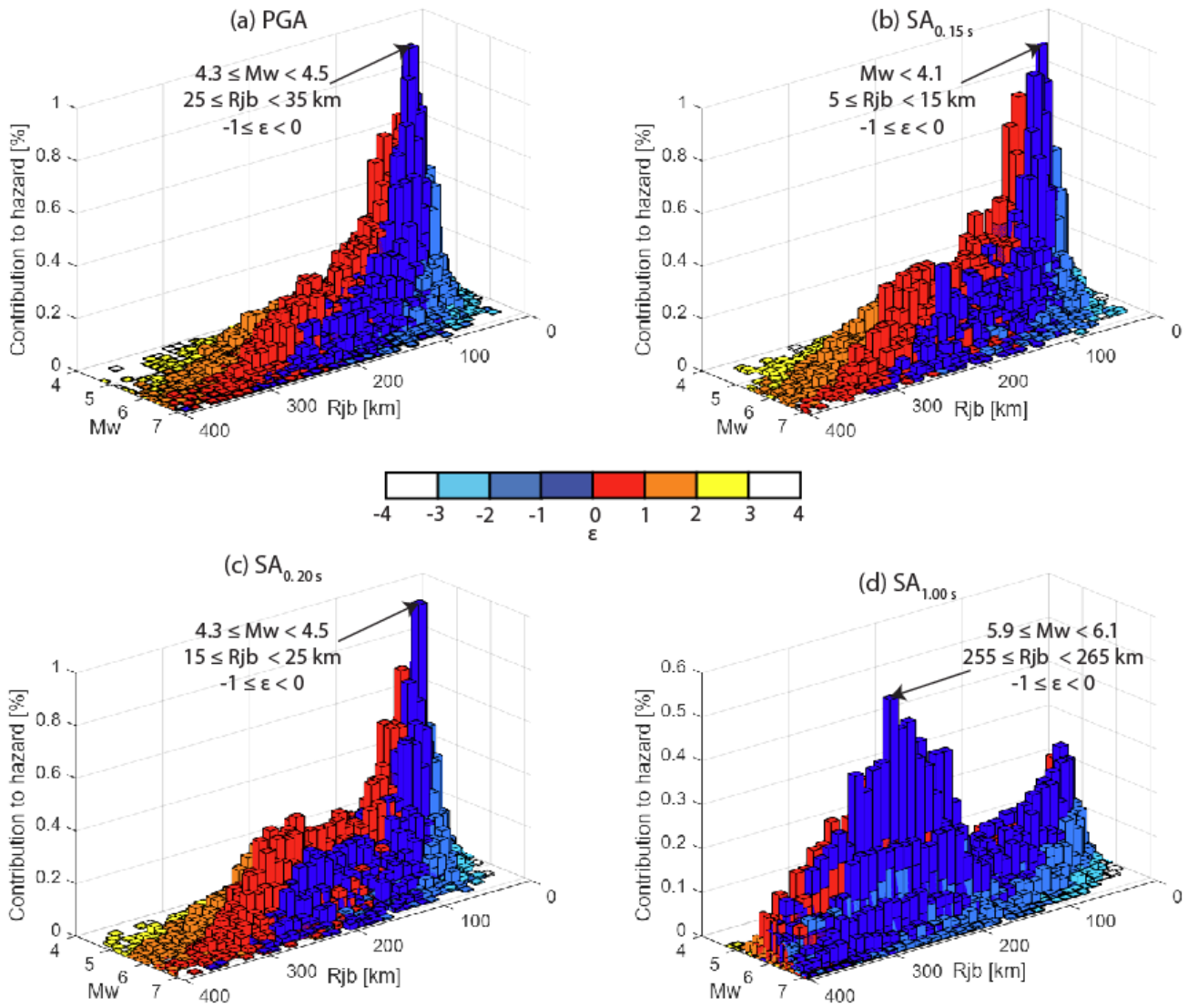


Figure 27 Disaggregation of the hazard for the Dover site and 475-year return period by magnitude (Mw), Joyner-Boore distance (Rjb) and epsilon (ϵ) for (a) PGA, (b) $SA_{0.2s}$, (c) $SA_{0.2s}$, and (d) $SA_{1.0s}$.

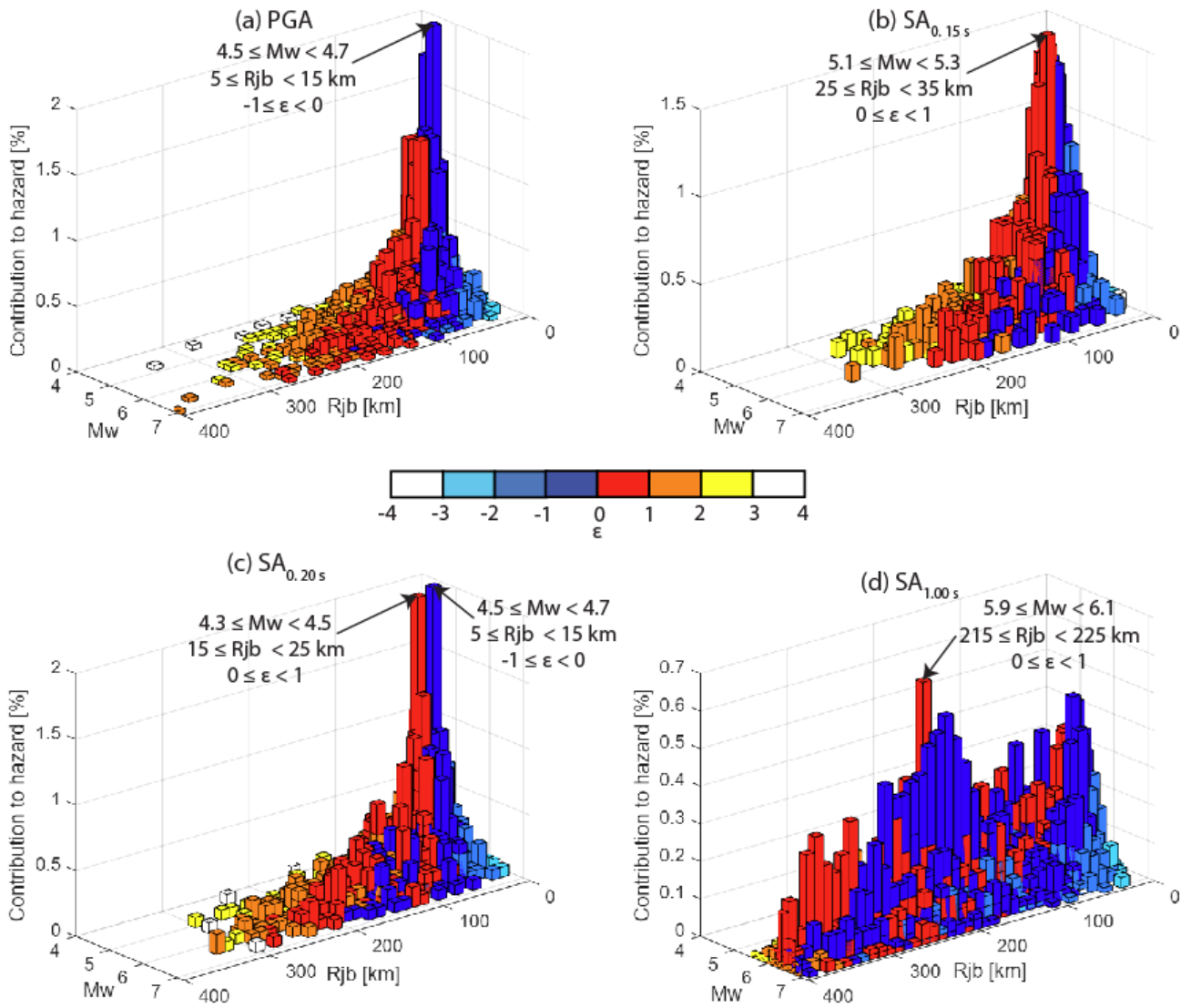


Figure 28 Disaggregation of the hazard for the Dover site and 2475-year return period by magnitude (Mw), Joyner-Boore distance (Rjb) and epsilon (ϵ) for (a) PGA, (b) $SA_{0.2s}$, (c) $SA_{0.2s}$, and (d) $SA_{1.0s}$.

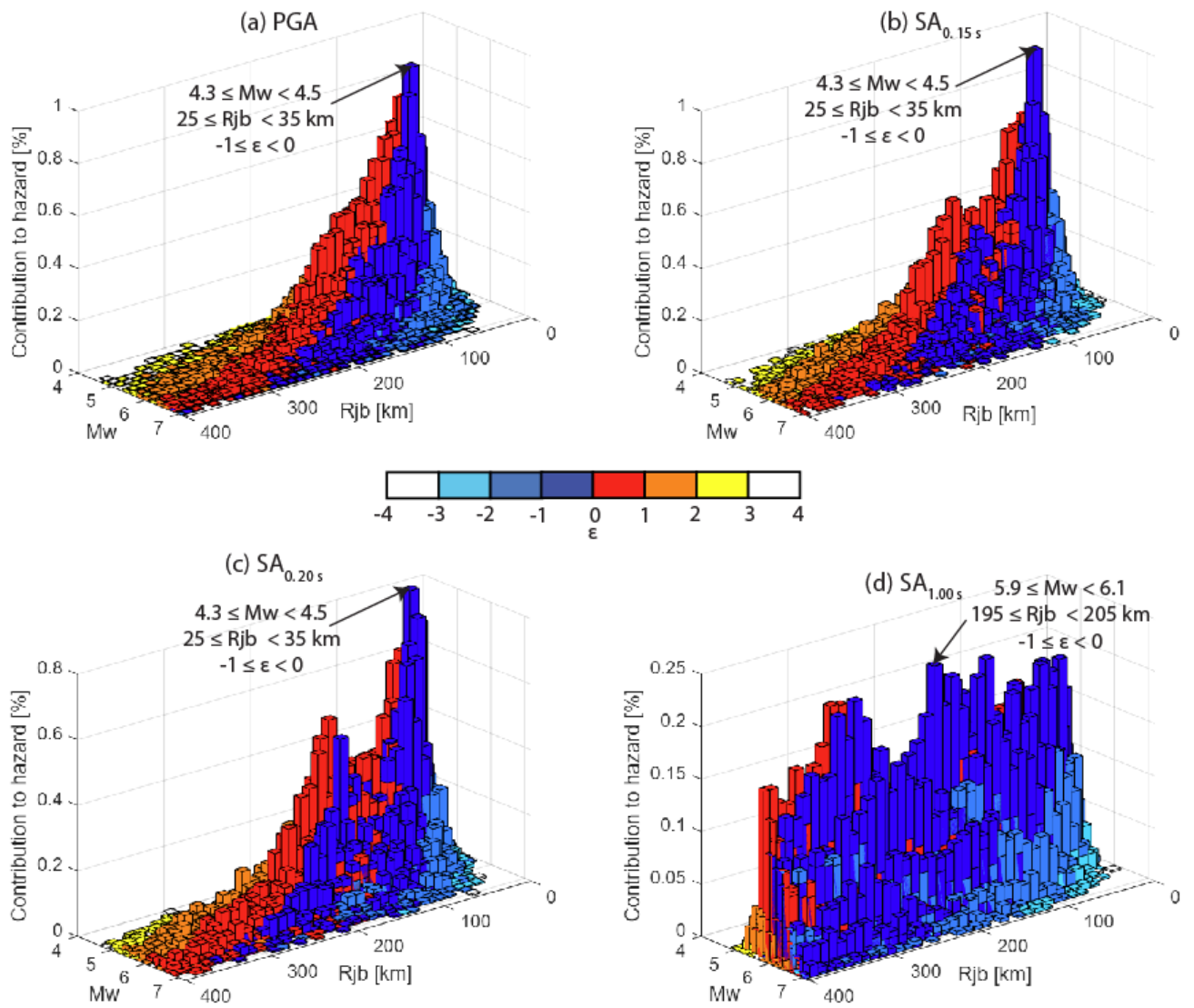


Figure 29 Disaggregation of the hazard for the Edinburgh site and 475-year return period by magnitude (Mw), Joyner-Boore distance (Rjb) and epsilon (ϵ) for (a) PGA, (b) $SA_{0.2s}$, (c) $SA_{0.2s}$, and (d) $SA_{1.0s}$.

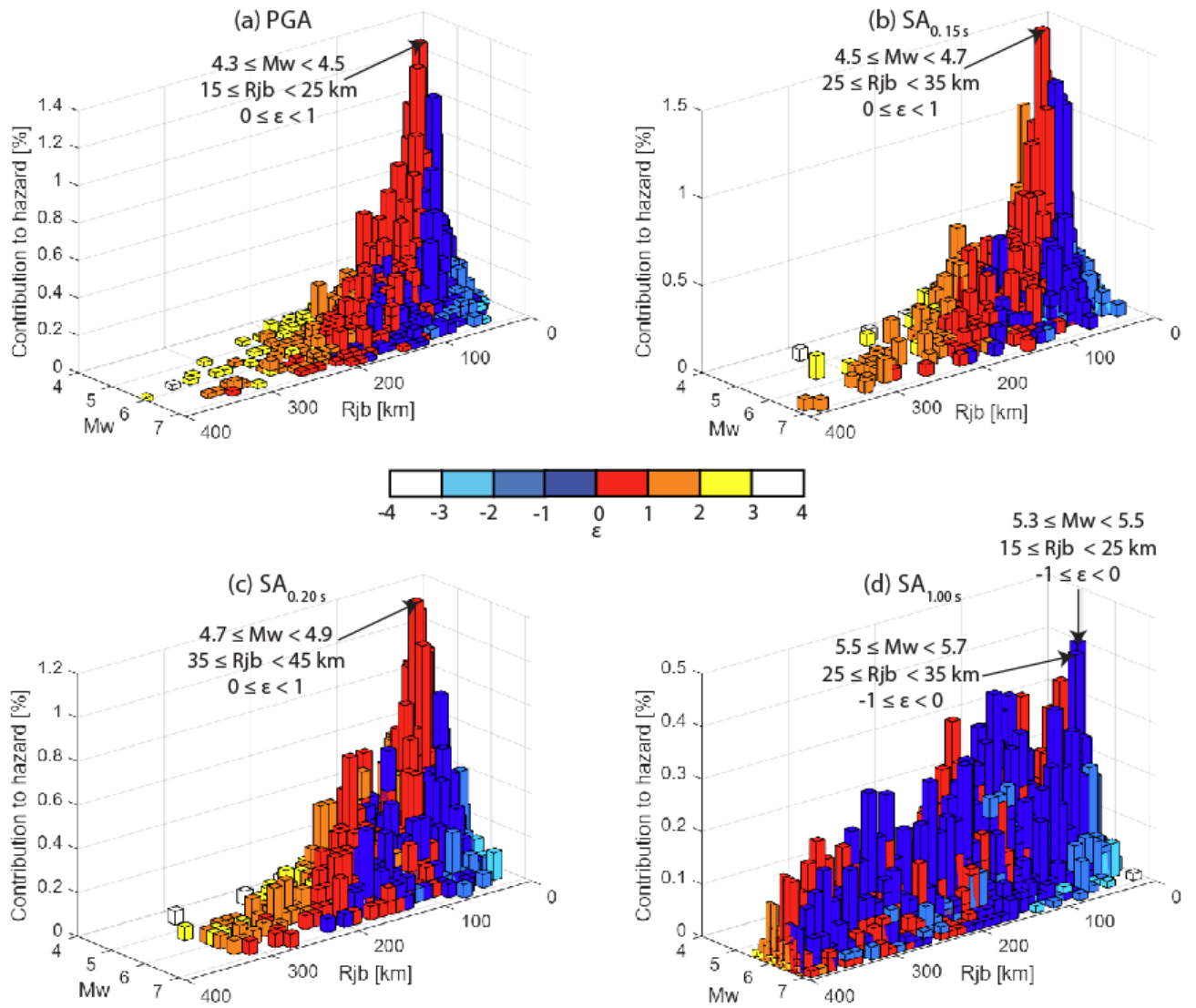


Figure 30 Disaggregation of the hazard for the Edinburgh site and 2475-year return period by magnitude (Mw), Joyner-Boore distance (Rjb) and epsilon (ϵ) for (a) PGA, (b) $SA_{0.2s}$, (c) $SA_{0.2s}$, and (d) $SA_{1.0s}$.

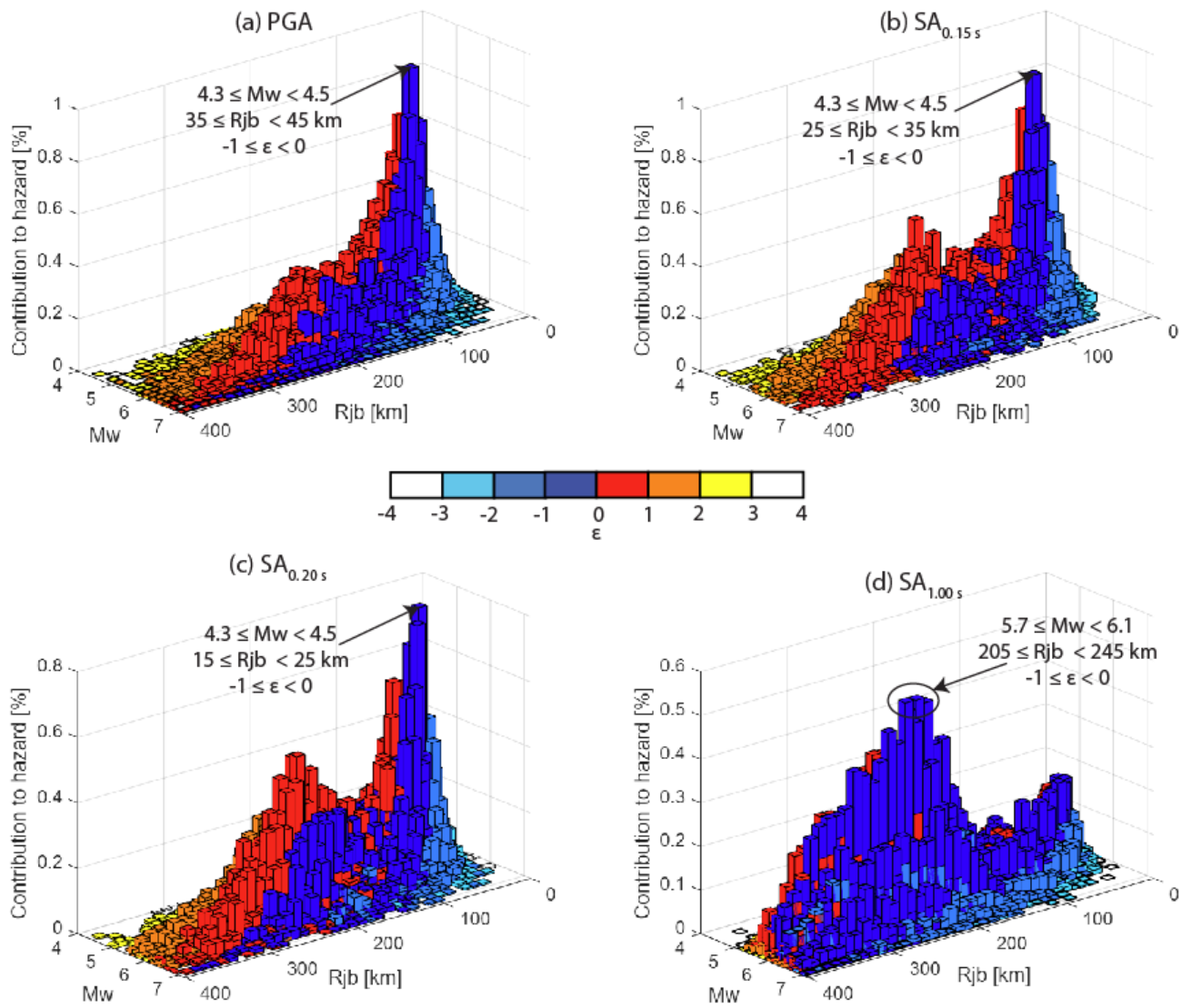


Figure 31 Disaggregation of the hazard for the London site and 475-year return period by magnitude (Mw), Joyner-Boore distance (Rjb) and epsilon (ϵ) for (a) PGA, (b) $SA_{0.2s}$, (c) $SA_{0.2s}$, and (d) $SA_{1.0s}$.

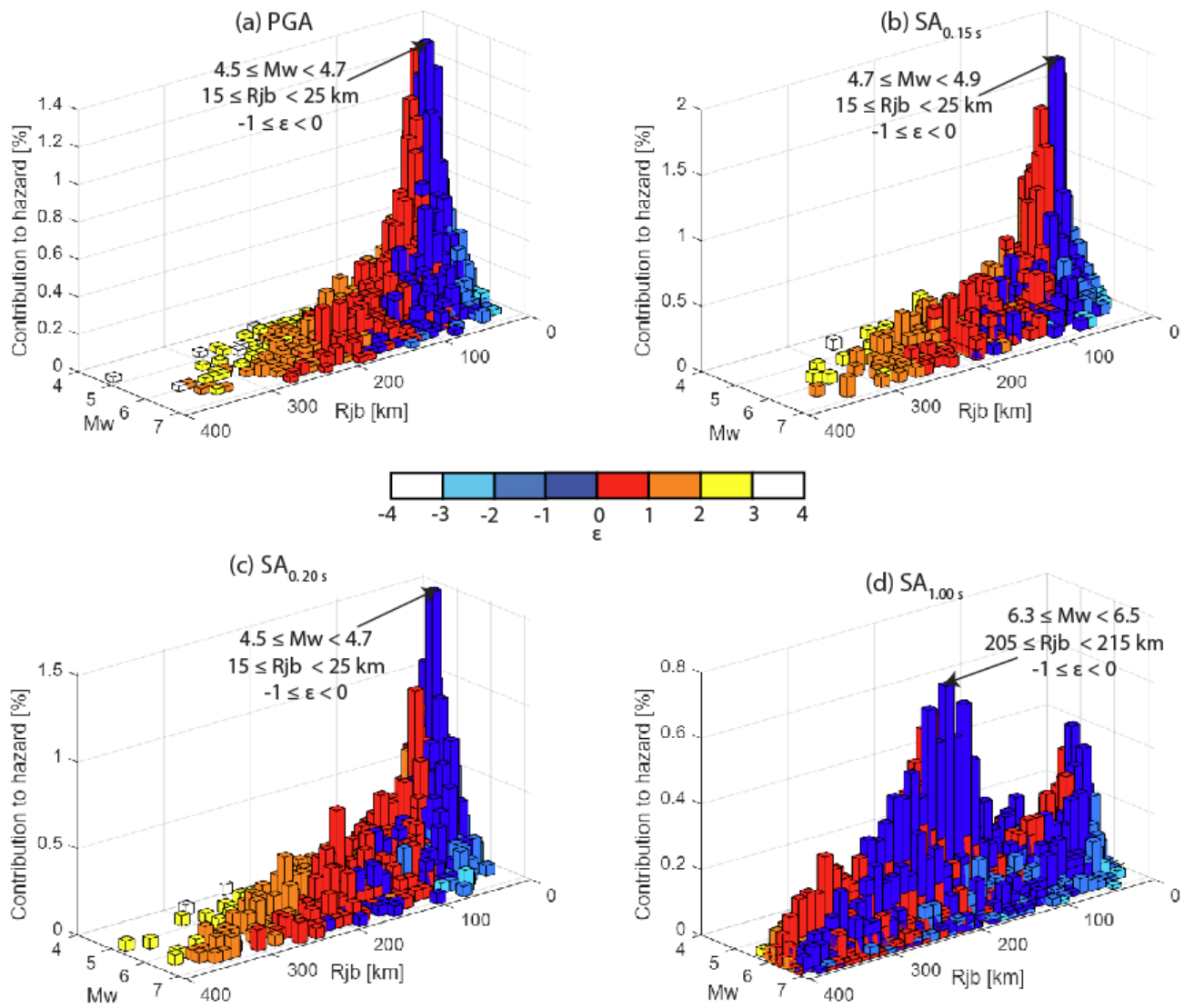


Figure 32 Disaggregation of the hazard for the London site and 2475-year return period by magnitude (Mw), Joyner-Boore distance (Rjb) and epsilon (ϵ) for (a) PGA, (b) $SA_{0.2s}$, (c) $SA_{0.2s}$, and (d) $SA_{1.0s}$.

Glossary

The definitions included in this section are taken directly from various sources: Reiter (1990), Budnitz et al. (1997), Stein and Wyssession (2003), McGuire (2004), PNNL (2014), and <https://earthquake.usgs.gov/learn/glossary/>.

Activity rate: The logarithm of the number of earthquakes of magnitude zero or greater expected to occur in a specific period of time, such as a year.

b-value: The slope of a straight line describing the Gutenberg-Richter recurrence frequency-magnitude law. It expresses the proportion of large earthquakes to small earthquakes.

Disaggregation: Statistical decomposition of the hazard to show the relative contribution by magnitude, distance, and ground motion deviation.

Earthquake: A phenomenon of fault rupture releasing stored strain in the Earth's crust and propagating from the source through vibratory waves in all directions.

Epicentre: The point of the earthquake on the Earth's surface.

Fault: A fracture surface or zone in the earth across which there has been relative displacement.

Ground motion model: See Ground motion prediction equation.

Ground motion prediction equation: An empirical model that relates a ground motion measure (e.g., peak ground acceleration and spectral acceleration) to a set of independent variables, such as distance, magnitude, source and path parameters. The GMPE predicts a lognormal distribution of values for the ground motion measure described by a median prediction and the standard deviation (sigma).

Gutenberg-Richter (recurrence) frequency-magnitude law: The relationship between magnitude and number of earthquakes in a given region and time period.

Hypocentre: The point in the earth at which an earthquake is initiated.

Joyner-Boore distance: The shortest distance from a site to the surface projection of the rupture surface of the earthquake.

Logic Tree: A series of branches to describe alternative models and parameter values. The weights, which must sum to unity at each node, are assigned to each branch using expert judgement that reflects the relative confidence in the models and parameters.

Magnitude: The size of the earthquake measured from the amplitude of the motion recorded on seismograms and expressed as a logarithm with base 10.

Maximum magnitude: The largest earthquake magnitude that a seismic source is capable of generating.

Moment magnitude: Magnitude derived from the scalar seismic moment.

Probabilistic seismic hazard analysis: A methodology to quantify the frequency of exceeding various ground motion levels at a site given all possible earthquakes in a probabilistic framework.

Peak ground acceleration: Maximum value of acceleration displayed on an accelerogram.

Rate of seismicity: Rate of occurrence of earthquakes above some specified magnitude for a specific region.

Return period: The mean (average) time between occurrences of a seismic hazard. It is the reciprocal of the annual frequency of exceeding a particular ground motion level.

Seismic hazard: Potential for dangerous, earthquake-related natural phenomena such as ground shaking, fault rupture, or soil liquefaction.

Seismic source: Region or volume (zone or fault) where the seismic activity is considered to be of homogeneous earthquake potential.

Seismic hazard curve: A graphical curve depicting the frequency (the number of events per unit time, usually a year) with which selected values of a ground motion measure are expected to be exceeded.

Seismic source model: Mathematical representation of the spatial and temporal distribution of expected earthquakes within a magnitude range in a specific region.

Seismic Source zone: Area where the seismic activity is considered to be of homogeneous earthquake potential, and earthquakes have an equal chance of occurring at any point in the zone.

Sigma model: Aleatory standard deviation in the ground motion model expressed in logarithms. It consists of the between-event standard deviation and the within-event standard deviation.

Strike-slip fault: A fault in which the relative displacement is along the strike of the fault plane, either right- or left-lateral.

Uncertainty: In seismic hazard analysis, there are two types of uncertainties: aleatory and epistemic uncertainty. The aleatory uncertainty is inherent in a random phenomenon and cannot be reduced by acquiring additional data or information. The future earthquake locations and magnitudes have aleatory uncertainty. The epistemic uncertainty is due to our lack of knowledge regarding the earthquake process, and it can be reduced by the accumulation of additional information. The geometry of the seismic source model and the maximum magnitude have epistemic uncertainty.

Vs30: Time-averaged shear wave velocity for the top 30 m.

References

The British Geological Survey holds most of the references listed and copies may be obtained via the library service subject to copyright legislation (contact libuser@bgs.ac.uk for details). The library catalogue is available at <https://ukrinerc.on.worldcat.org/discovery>

- Abrahamson, NA, Silva, WJ, and Kamai, R. 2014. Summary of the ASK14 ground motion relation for active crustal regions. *Earthquake Spectra*, Vol. 30(3):1025–1055. DOI: <https://doi.org/10.1193/070913EQS198M>.
- Al Atik, L. 2015. NGA-East: Ground-Motion Standard Deviation Models for Central and Eastern North America. *PEER Report, No. 2015/07* (Berkeley, California: Pacific Earthquake Engineering Research Center).
- Atkinson, GM, and Boore, DM. 2006. Earthquake ground motion prediction equations for eastern North America. *Bulletin of the Seismological Society of America*, Vol. 96(6):2181–2205. DOI: <https://doi.org/10.1785/0120050245>.
- Baptie, B. 2010. State of stress in the UK from observations of local seismicity. *Tectonophysics*, Vol. 482, 150-159. DOI: <https://doi.org/10.1016/j.tecto.2009.10.006>.
- Bindi, D, Massa, M, Luzi, L, Ameri, G, Pacor, F, Puglia, R, and Augiera, P. 2014. Pan-European ground-motion prediction equations for the average horizontal component of PGA, PGV, and 5%-damped PSA at spectral periods up to 3.0 s using the RESORCE dataset. *Bulletin of Earthquake Engineering*, Vol. 12(1), 391–430. DOI: <https://doi.org/10.1007/s10518-013-9525-5>.
- BS NA EN 1998-1 (2008). UK National Annex to Eurocode 8: Design of structures for earthquake resistance. *British Standards Institution*, Chiswick (United Kingdom).
- PD6698. 2026. Published document - Recommendations for the design of structures for earthquake resistance to BS EN 1998. *British Standards Institution*, Chiswick (United Kingdom).
- Cauzzi, C, Faccioli, E, Vanini, M, and Bianchini, A. 2015. Updated predictive equations for broadband (0.01–10s) horizontal response spectra and peak ground motions, based on a global dataset of digital acceleration records. *Bulletin of Earthquake Engineering*, Vol. 13, 1587–1612. DOI: <https://doi.org/10.1007/s10518-014-9685-y>.
- Danciu, L, Giardini, D, Weatherill, G, Basili, R, Nandan, S, Rovida, A, Beauval, C, Bard, P-Y, Pagani, M, Reyes, C, Sesetyan, K, Vilanova, S, Cotton, F, and Wiemer, S. 2024. The 2020 European Seismic Hazard Model: Overview and Results. *EGU Sphere*, DOI: <https://doi.org/10.5194/nhess-24-3049-2024>.
- Douglas, J, and Edwards, B. 2016. Recent and future developments in earthquake ground motion estimation. *Earth-Science Review*, Vol. 160, 203–219. DOI: <https://doi.org/10.1016/j.earscirev.2016.07.005>.
- EN 1998. 2005. Eurocode 8: Design of structures for earthquake resistance. European Committee for Standardization, Brussels, Belgium.
- EN 1998. 2026. Eurocode 8: Design of structures for earthquake resistance. European Committee for Standardization, Brussels, Belgium.
- EQE International Ltd. 2002. Seismic hazard - UK continental shelf (2002). *Offshore Waters Report HSE-OTR OTH-2002/005*, UK and Health and Safety Executive, London, UK.
- Gibson, J. 2009. The United Kingdom's elusive exclusive economic zone. *Journal of Water Law*, Vol. 20, 179-185.
- IAEA. 2022. Seismic Hazards in Site Evaluation for Nuclear Installations. *IAEA Specific Safety Guide Series No. SSG-9* (Vienna, Austria: International Atomic Energy Agency).
- Johnston, AC, Coppersmith, KJ, Kanter, LR, and Cornell, CA. 1994. The earthquakes of stable continental regions, *Electric Power Research Institute Report* (Palo Alto, California: Electric Power Research Institute).
- Lindholm, CD, Bungum, H, Hicks, E, and Villagran, M. 2000. Crustal stress and tectonics in Norwegian regions determined from earthquake focal mechanisms. Vol. 167, 429-440 in *Dynamics of the Norwegian Margin*. Nøttvedt, A (Editor). (London, United Kingdom: Geological Society, Special Publications). DOI: <https://doi.org/10.1144/GSL.SP.2000.167.01.17>.
- Mosca, I. In preparation. Why do recent seismic hazard models for the UK region produce different results? *Bulletin of Earthquake Engineering*.
- Mosca, I, Sargeant, S, Baptie, B, Musson, RMW, and Pharaoh, T 2020. National seismic hazard maps for the UK: 2020 update. *British Geological Survey Open Report*, OR/20/053 (Nottingham, United Kingdom: British Geological Survey).
- Mosca, I, Sargeant, S, Baptie, B, Musson, RMW, and Pharaoh, T 2022. The 2020 national seismic hazard model for the United Kingdom. *Bulletin of Earthquake Engineering*, Vol. 20, 633–675. DOI: <https://doi.org/10.1007/s10518-021-01281-z>.
- Mosca, I, Baptie, B, Haslam, R, Gafeira, J, and Jenkins, G. 2024. Seismic Hazard Assessment for the UK Offshore Exclusive Economic Zone. *British Geological Survey Open Report*, OR/24/012 (Nottingham, United Kingdom: British Geological Survey).

- Musson, RMW. 2000. The use of Monte Carlo simulations for seismic hazard assessment in the UK. *Annali di Geofisica*, Vol. 43, 1-9. DOI: <https://doi.org/10.4401/ag-3617>.
- Ottmøller, L, Nielsen, HH, Atakan, K, Braunmiller, J, Havskov, J. 2005. The 7 May 2001 induced seismic event in the Ekofisk oil field, North Sea. *Journal of Geophysical Research*, Vol. 110(B10), B10301. DOI: <https://doi.org/10.1029/2004JB003374>.
- Rietbrock, A, Strasser, FO, and Edwards, B. 2013. A stochastic earthquake ground motion prediction model for the United Kingdom. *Bulletin of the Seismological Society of America*, Vol. 103(1), 57-77.
- Rietbrock A, and Edwards, B. 2019. Update of the UK stochastic ground motion model using a decade of broadband data. *SECED 2019 Conference*, Greenwich, United Kingdom.
- Yenier, E, and Atkinson, GM. 2015. Regionally adjustable generic ground-motion prediction equation based on equivalent point-source simulations: Application to central and eastern North America. *Bulletin of the Seismological Society of America*, Vol. 105, 1898–2009. DOI: <https://doi.org/10.1785/0120140332>.